Tumor-specific Delivery of Anticancer Nucleic Acids by Anti-EGF Receptor Immunonanoparticles

Jung Seok Kim

The Graduate School
Yonsei University
Department of Biomedical
Laboratory Science

Tumor-specific Delivery of Anticancer Nucleic Acids by Anti-EGF Receptor Immunonanoparticles

A Dissertation Submitted to Department of Biomedical Laboratory Science and the Graduate School of Yonsei University in Partial Fulfillment of the Requirement for the Degree of Doctor of Philosophy

Jung Seok Kim

July 2012

This certifies that the dissertation of Jung Seok Kim is approved.

Thesis Supervisor : Yong Serk Park

Ok Doo Awh : Thesis Committee Member

Jong Bae Kim : Thesis Committee Member

Hyeyoung Lee : Thesis Committee Member

Hong Sung Kim : Thesis Committee Member

The Graduate School

Yonsei University

July, 2012

"They that hope in the LORD will renew their strength, they will soar as with eagles' wings; They will run and not grow weary, walk and not grow faint."
(Isaiah 40:31)

CONTENTS

LIST OF FIGURES

LIST OF TABLES

ABBREVIATIONS

AAV : Adeno-associated virus
Chol : Cholesterol
CMV : Cytomegalovirus
CSV : Cationic Sendai F/HN Viroplexes
DMKE : O,O'-dimyristyl-N-lysyl glutamate
DSPE-PEG_{2000} : 1,2-distearoyl-sn-glycero-3-phosphoethanolamine-N-[methoxy(polyethylene glycol)2000]
DSPE-PEG_{2000}-MAL : 1,2-distearoyl-sn-glycero-3-phosphoethanolamine-N-[maleimide(polyethylene glycol)2000]
EDTA : Ethylenediaminetetraacetic acid
EGFR : Epidermal growth factor receptor
F/HN : Sendai viral fusion/hemagglutinin neuraminidase protein
Luc : Luciferase
MFI : Mean of fluorescence intensity
PEG : Polyethylene glycol
PI : Propidium iodide
pIL12 : Plasmid IL12 DNA
PILs : Pegylated immunoliposomes
PILPs : Pegylated immunolipoplexes
PBS : Phosphate-buffered saline
POPC : 1-palmitoyl-2-oleoyl-sn-glycero-3-phosphocholin
PS : Protamine sulfate
pSal : Plasmid salmosin DNA
Rho-DOPE : 1,2-dioleoyl-sn-glycero-3-phosphoenthanolamine-N-[lissamine rhodamine B sulfonyl]
RLU : Relative light unit
SDS-PAGE : Sodium dodecyl sulfate-polyacrylamide-gel electrophoresis
siRNA : Small-interfering RNA

Abstract

Tumor-specific Delivery of Anticancer Nucleic Acids by Anti-EGF Receptor Immunonanoparticles

Department of Biomedical Laboratory Science
The Graduate School, Yonsei University

Cancer gene therapy is the treatment of cancers by transferring therapeutic genes (plasmid DNA, micro RNA or small interfering RNA) with gene delivery systems. The drawbacks of gene delivery systems in the issues of safety and transfection efficiency make their clinical applications difficult. Liposomal gene delivery systems have been considered to be relatively safer, less immunogenic and non-infectious than viral gene delivery systems. Typically, cationic liposomes have been widely utilized for *in vitro* and *in vivo* gene transfection because of easy and stable formation of liposome-DNA complexes called lipoplexes. In recent years, the liposomal gene delivery systems have been improved in terms of transfection efficiency and stability *in vivo*. For example, virosomes, fusogenic viral envelop proteins reconstituted in liposomal vesicles, were more effective in transfection to various cells and tissues than other conventional cationic lipoplexes. However, gene transfection efficiency of liposomal systems still needs to be further improved for clinical applications. In this study, anti-epithermal growth factor receptor (EGFR) immunonanoparticles (immunoliposomes, immunovirosomes, immunolipoplexes and immunoviroplexes) were developed for EGFR-directed gene delivery to cancer cells. The four different types of EGFR-targeted liposomal systems were finally constructed by conjugation of Cetuximab, anti-EGFR monoclonal antibody, to PEG termini on the liposomal surface. The resulting anti-EGFR antibody-conjugated immunonanoparticles were able to effectively deliver

genes (pDNA and siRNA) to EGFR-positive cancer cells (A549 and SK-OV-3 cells), but not to EGFR-negative ones (MCF-7 and B16BL6). Especially, the anti-EGFR immunoviroplexes exhibited the most efficient transfection to EGFR-expressing tumor cells than the others. The anti-EGFR immunonanoparticles were able to more selectively deliver to SK-OV-3 tumors xenografted in mice than conventional cationic DMKE/Chol lipoplexes. The two different types of anticancer genes (pDNA; IL12 gene and/or salmosin gene, siRNA; vimentin siRNA and/or JAK3 siRNA) were encapsulated in anti-EGFR immunolipoplexes and anti-EGFR immunoviroplexes and then intravenously injected to the SK-OV-3 tumor-xenografted mouse model. The gene transfected mice were also treated with anti-cancer drug, doxorubicin. According to the experimental data, the anti-EGFR immunonanoparticles containing both types of anticancer genes were more effective in inhibition of tumor growth and metastasis. In addition, the combined treatment with doxorubicin was able to synergistically inhibit SK-OV-3 tumor growth in mice. Among the anti-EGFR immunononoparticles, the anti-EGFR immunoviroplexes exhibited the most efficient EGFR-specific transfection, resulting in the most effective therapeutic efficacy. This study suggests that the anti-EGFR immunonanoparticles, specially the anti-EGFR immunoviroplex formulation, would be useful as an efficient tumor-specific gene delivery system for cancer gene therapy. Also, combination of conventional chemotherapy and tumor-directed anticancer gene therapy can be an acceptable modality for anticancer therapy.

Key words : gene therapy, anti-EGFR immunonanoparticle, immunoliposome, immunolipoplex, immunovirosome, immunoviroplex, EGFR, Cetuximab, Sendai F/HN protein, IL12 gene, salmosin gene, vimentin siRNA, JAK siRNA

PART I

Tumor-specific anticancer gene delivery by anti-EGFR immunonanoparticles

Ⅰ. INTRODUCTION

Gene therapy is becoming a promising approach for the treatment of diseases such as hereditary or acquired diseases. Recently, more gene therapy studies are aimed at cancer treatment. Cancer gene therapy can be defined as cancer treatment by transferring anti-tumoral plasmid DNA (pDNA), micro RNA (miRNA) or small interfering RNA (siRNA) with gene delivery systems (1). However, the lack of safe and efficient gene delivery systems makes their clinical application difficult at this moment.

There are two different types of gene delivery strategies for gene transferring to cancer cells, gene transfection mediated by viral vector or non-viral vector systems. Viral vectors have shown higher transaction efficiency and long-term gene expression than nonviral vectors. Hence, viral vectors, such as adenoviruses, adeno-associated viruses, and retroviruses including lentiviruses have been considered to be promising gene delivery carriers. However, the viral vectors have been reported to have serious side-effects, such as toxicity, immunogenicity and inflammatory responses in host cells, limited loading capacity, and difficulties in large-scale production (2). Therefore, nonviral vectors, such as liposomal vectors (liposomes or virosomes), cationic peptides or cationic polymers, have recently received increasing attention as gene delivery systems (3). Non-viral vectors have become widespread because of their capacity to transfer large-scale genes, site-specific transfer, and their less immunogenic, non-toxic and non-infectious properties. However, the clinical usefulness of non-viral methods is also limited by their low transfection efficiency and relatively poor transgene expression (4).

Cancer is still a severe uncontrollable disease with high rates of morbidity and mortality although many therapeutic treatments have been developed. Generally, cancer treatment includes the surgical removal of cancer lesions along with the surrounding normal tissues, followed by chemotherapy and radiotherapy. However, in many cases the cancer cells are not completely eliminated from the body, which allows the tumors to recur (5). To suppress the growth of residual cancer after surgery of malignity cancers, numerous

anticancer drugs, reagents or therapeutic procedures have been developed.

The tumor specific molecular targets for cancer diagnostics and therapy has led to the specific detection and treatment of cancer cells in several types of cancer (6, 7). The concept of targeted drug or gene delivery was proposed by Paul Ehrlich in 1906 as a 'magic bullet' (8), and the tumor-specific delivery system for cancer was developed more after when Bangham defined liposomes (9). Thus, tumor cells can be specifically detected based on characteristic alterations in oncogene expressed products and other specific molecules as a key. Oncogene products can therefore be used as targets for diagnosis, imaging and therapy (6).

The epidermal growth factor receptor (EGFR) has been recognized as a therapeutic target molecule for cancer treatment. It is a cell surface receptor over-expressed in several cancers such as breast, ovarian, lung, head and neck, prostate, and colorectal cancers, and have been proposed as a prognostic marker for cancer progression and survival (10). Preclinical and clinical studies have shown that targeting the epidermal growth factor receptor (EGFR) family is a valid strategy for diagnosis and anticancer therapy (11-12). The EGFR family is the prototypic member of the class I family of receptor tyrosine kinases, which includes EGFR, HER2 (ErbB2), HER3 (ErbB3) and HER4 (ErbB4) (13). The EGFR expressed on the cell surface is activated by binding of its specific ligands including epidermal growth factor and transforming growth factor α (TGFα).

Dysregulation of EGFR signaling has been known to contribute to malignant transformation of cells. As a target antigen, EGFR is a readily accessible cell surface receptor. When over-expressed, provides a basis for selective antibody-based targeting of varied types tumor cells (14). Consequently, strategies targeting EGFR have been developed as a treatment option, including monoclonal antibodies, small molecule inhibitors of EGFR-mediated signal transduction, and antibody-based immunoconjugates. Some of these reagents have already been approved for cancer therapy such as monoclonal antibodies (Cetuximab, Panitumumab) and small molecule inhibitors (Gefitinib®, Erlotinib®). Actually, monoclonal antibodies (MAbs) against EGFR such as Cetuximab can inhibit the proliferation of EGFR-overexpressing cells *in vitro* and in tumor xenograft models (15-18).

Liposomal gene delivery systems such as liposomes and virosomes have been used as sustained-action delivery vectors for a wide variety of vaccines, drugs and genetic oligonucleotides (DNA or RNA). Among various liposomal nanoparticles used as drug or gene delivery systems, liposomes are the most well studied materials because of their amphiphilic and biocompatible characteristics (19, 20). Liposome are composed of vesicular lipid bilayers surrounding a large inner aqueous phase. Various therapeutics are encapsulated into the liposomes, which eventually break down through natural processes and release their contents into the bloodstream or into nearby tissues.

Cationic liposomes have been established as one of non-viral gene delivery systems for studies and clinical purposes. Cationic liposomes are able to easily and rapidly prepare cationic liposomes-DNA complexes (called lipoplexes) via charge interaction. Cationic lipoplexes have relatively high transfection efficiency *in vitro* or when locally delivered at low doses (21). Complexed DNA is strongly compacted and protected from lytic enzymes (22). Also, because of their surface charge they interact with the cell membranes, then internalized via endocytosis. Therefore, cationic lipoplexes have the potential to deliver intracellular large polynucleic acid molecules. However, their *in vivo* transfection sites are limited to the lung and liver because of their large size, excessive positive charge and considerable aggregation property (23, 24).

Virosomes are chimeric gene transfer system combining viral and non-viral features due to the viral constituents of envelop proteins and artificial liposomal vesicles. Among the chemical delivery systems, the virosomes are known to be one of the most effective transfection systems. Therefore, many different types of virosomes have been formulated from several enveloped viruses including influenza, HSV, HIV, and Sendai virus (25).

To enhance transfection efficiency of nonviral vectors, target-specific gene delivery has been continuously explored (26). In recent years, a variety of target-specific liposomal systems have been developed adopting various targeting ligands such as cell-specific antibodies, peptides and other small ligands. It has been demonstrated that specific delivery of genes to the target cells is far more efficient with immunoliposomes or immunolipoplexes than

with conventional bare liposomes or lipoplexes lacking antibody (26). The therapeutic advantages of liposomal immunonanoparticles include the targeting ability to deliver a large amount of encapsulated drugs to specific target sites, resulting in improved drug pharmacokinetics and gene transfection efficacy and reduced cellular toxicity (27-29).

One of the drawbacks of conventional liposomes is that it can be easily cleared and enhanced uptake of nanoparticles by the reticular endothelial system (RES) resulting in a reduced targeting yield (30-32). This can be overcome by modifying the liposome surface with flexible hydrophilic polymers such as polyethylene glycol (PEG) to produce so-called "stealth" liposomes (33-35). The increased circulation longevity of the PEG-liposomes allow enhanced extravasation across the leaky endothelium of solid tumors (36, 37).

Salmosin, a novel disintegrin derived snake (*Gloydius saxatilis*) venom, is a single-chain polypeptide composed of 73 amino acids, including 12 cysteines and an RGD(Arg-Gly-Asp) sequence (38). In previous studies, it has been reported that salmosin strongly inhibited tumor growth by suppression of angiogenesis without affecting the normal proliferation of endothelial cells (39). IL12 is a well-known immunostimulatory cytokine that has been reported as a potential anticancer agent (40). It has been also known to activate NK cells as well as cytotoxic T cells to promote Th1 immune responses (41), and to inhibit tumor growth and angiogenesis (42). There are many studies that recombinant IL12 proteins have been tested in preclinical and clinical trials. However, the IL12 treatment showed significant toxicity in a phase I clinical trial (43).

Based on the urgent demands in the field of nonviral gene delviery, the present study was designed to develop a target-directed liposomal gene delivery system for enhanced gene transfection to tumor cells. Four different types of anti-EGFR (epithermal growth factor receptor) immunonanoparticles (immunoliposomes, immunovirosomes, immunolipoplexes and immunoviroplexes) were prepared for intracellular gene delivery targeted to EGFR-overexpressing tumor cells. The anti-EGFR immunonanoparticles were evaluated in terms of their binding affinities to EGFR-overexpressing tumor cells. Also, their gene-transferring capabilities were compared with conventional cationic

lipoplexes *in vitro* and *in vivo*. Anticancer genes (pDNA; IL12 gene and/or salmosin gene, siRNA; vimentin siRNA and/or JAK3 siRNA) were delivered using the immunonanoparticles and their anti-tumoral effects were systematically compared to each other. The all experimental evidence suggested which immunonanoparticles are an appropriate system for EGFR-targeted gene therapy.

Ⅱ. MATERIALS AND METHODS

1. Materials

1-palmitoyl-2-oleoyl-sn-glycero-3-phosphocholin (POPC), 1,2-distearoyl-sn-glycero-3-phosphoethanolamine-N-[methoxy(polyethyleneglycol)2000] (DSPE-PEG2000), 1,2-distearoyl-sn-glycero-3-phosphoethanolamine-N-[maleimide (polyethyleneglycol)2000] (DSPE-PEG2000-MAL), cholesterol, 1,2-dioleoyl-sn-glycero-3-phosphoenthanolamine-N-[lissamine rhodamine B sulfonyl] (Rho-DOPE) were purchased from Avanti Polar Lipid, Inc. (Alabaster, USA). PD-10 column and sepharose CL-4B were purchased from Amersham Bioscience (Uppsala, Sweden). Amicon Ultra-4 30K and 50K MWCO were purchased from Amicon (Beverly, Sweden). O,O'-dimyristyl-N-lysyl glutamate (DMKE) cationic lipid was chemically synthesized by Dr. Jang (Department of Chemistry and Medicinal Chemistry, Yonsei University, Korea).

2. Cells and cell culture

Human ovarian adenocarcinoma SK-OV-3 (No. HTB-77), lung adenocarcinoma A549 (No. CCL-185), and breast carcinoma MCF-7 cells (No. HTB-22) were purchased from the American Type Culture Collection (Manassas, USA). Mouse melanoma B16BL6 cells were developed by Dr. I. J. Fidler at MD Anderson Cancer Center (Houston, USA). SK-OV-3 cells were maintained as monolayer cultures in DMEM/F12 (Gibco, Carlsbad, USA), A549 cells in RPMI 1640, MCF-7 cells in DMEM, and B16BL6 cells in MEM. SK-OV-3 and A549 cells are EGFR-positive cell lines while MCF-7 and B16BL6 cells are not. The culture media were supplemented with 10% heat-inactivated fetal bovine serum (Gibco) and 100 units/㎖ penicillin and 100 ㎍/㎖ streptomycin (Gibco). The all cancer cells were cultured in a humidified atmosphere of 95% air and 5% CO_2 at 37℃.

3. Plasmid preparation

The luciferase-encoding plasmid pAAVCMV-Luc (pLuc), mouse interleukin 12-encoding plasmid pAAVCMV-mIL12 (pIL12) and salmonsin-encoding plasmid pFLAG-Sal (pSal) were propagated in DH5α strain of *E. coli* under selective LB (Luria-Bertani) media with ampicillin. The plasmids were isolated and purified by a Plasmid Mini-prep Kit (spin-type) (Elpis, Taejeon, Korea). Purity of the isolated plasmid was confirmed by 1% agarose gel electrophoresis and their DNA concentrations were measured by UV-spectrophotometer (Amersham Bioscience, Uppsala, Sweden).

4. Preparation of Sendai viral F/HN proteins

A suspension of 10 mg of Sendai virus (ATCC No. 1698936, VR 907) in PBS was centrifuged at 100,000 g for 1 h at 4℃. The pellet was resuspended in 2 ml of PBS containing 1% Triton X-100. After incubation at 20℃ for 2 h, the suspension was centrifuged at 100,000 g for 1 h at 4℃ to remove the detergent-insoluble substances presumably containing nucleocapsids. The detergent was removed from the clear supernatant by stepwise addition of SM2 Bio-Beads (Bio-Rad Lab., Hercules, USA) with constant rocking. Initially, the supernatant was incubated with 100 mg of methanol-washed SM2 Bio-Beads at room temperature. Two hours later, additional 100 mg of SM2 Bio-Beads were added to the reaction solution, which was further incubated at room temperature for 2 h. Another 200 mg of SM2 Bio-Beads were added and the incubation was terminated 2 h later. The turbid suspension was separated from the Bio-Beads using a 26-gauge needle. For purification of the F protein, the HN proteins were removed by dithiothreitol treatment before addition of Triton X-100. The virus pellet was resuspended in 4 ml of PBS containing 3 mM dithiothreitol. The suspension was incubated at 37℃ for 4 h and then dialyzed at 4℃ for 16 h against three changes of 1 l of PBS. The viral particles were centrifuged at 100,000 g for 1 h at 4℃ and the pellet was resuspended in 2 ml of PBS containing Triton X-100. After incubation at 20℃ for 2 h, the detergent was removed following the same procedure described above.

5. Preparation of immunonanoparticles

5-1. Preparation of liposomes and virosomes encapsulating plasmid DNA

DMKE (5 mole%), POPC (91 mole%), DSPE-PEG_{2000} (3.8 mole%), DSPE-PEG_{2000}-MAL (0.2 mole%) and Rho-DOPE (0.1 mole%) were dissolved in chloroform and methanol mixture (2:1, v/v). The organic solvent was evaporated under a stream of N_2 gas. Vacuum desiccation for 2 h ensured removal of the residual organic solvent. The dried films of 2 mg lipids were hydrated in 1 ml of 0.1 M phosphate buffer (pH 5.5) containing pDNA (10:1, lipid wt:pDNA wt) and then vigorously mixed by a vortex mixer for 5 min. After hydration, the liposomes were repeated 10 cycles freezing and thawing, and extruded 10 times through a polycarbonate membrane with a pore size from 800 nm to 80 nm using a extruder (Avanti Polar Lipids, Alabaster, USA). In order to prepared virosomes, after incubation of the extruded liposomes for 30 min at room temperature, Sendai viral F/HN proteins (1:1, pDNA wt:F/HN protein wt) were added and incubated for 15 min at room temperature with tapping. Then, the buffer was changed to phosphate buffer (0.1 M, pH 7.2).

5-2. Preparation of cationic liposomes and cationic virosomes

DMKE (48 mole%), cholesterol (48 mole%), DSPE-PEG_{2000} (3.8 mole%), DSPE-PEG_{2000}-MAL (0.2 mole%) and Rho-DOPE (0.1 mole%) were dissolved in the chloroform and methanol mixture (2:1, v/v). The organic solvent was evaporated under a stream of N_2 gas. Vacuum desiccation of 2 h ensured removal of the residual organic solvent. The dried lipid films (2 mg lipid) were hydrated in 1 ml of 0.1M phosphate buffer (0.1 M, pH 7.2) and then vigorously mixed by vortexing. After hydration, the resulting suspension was subjected to 10 cycles of freezing and thawing, and extruded 10 times through a polycarbonate membrane with a pore size of 80 nm using a extruder. Protamine sulfate (PS) condensed DNA-encapsulating cationic lipoplexes and viroplexes were prepared by pre-complexation of plasmid DNA with PS (Sigma, St. Louis, USA) (1:1, DNA wt:PS wt) for 30 min at room temperature. Lipoplexes (DNA-liposome complexes) were prepared by gentle mixing of PS-condensed plasmid DNA and the cationic liposome (DMKE/Chol) solution at various N/P ratios of DNA/lipid. After incubation for 30 min at room temperature, Sendai viral F/HN proteins (1:1, DNA wt:F/HN protein wt) were added and incubation continued 15 min at room temperature with gentle mixing. The resulting complex is called viroplexes.

5-3. Thiolation of anti-EGFR antibody

Cetuximab (Erbitux®, Imclone, USA) were thiolated for 1 h at room temperature by reacting with Traut's reagent in degassed phosphate buffer (0.1 M, 2 mM EDTA, pH 8.0). Unreacted Traut's reagent was removed by passing through PD-10 column with the degassed phosphate buffer.

5-4. Conjugation of anti-EGFR antibody to nanoparticles

Neutral liposomes consisting of DMKE:POPC:DSPE-PEG_{2000}:DSPE-PEG_{2000}-MAL:Rho-DOPE and cationic liposomes consisting of DMKE:Chol:DSPE-PEG_{2000}:DSPE-PEG_{2000}-MAL:Rho-DOPE were prepared by the lipid extrusion method described above. The thiolated antibodies were conjugated to the maleimide moiety at the distal-termini of PEG chains on the nanoparticles. Briefly, the solution of thiolated antibody was added to the liposome and lipoplex solutions (0.2:1, mole ratio of Ab and maleimide), and then incubated for 20 h at 4℃ with continuous rocking. Unconjugated antibodies were separated from the nanoparticle solution by chromatography through a Sepharose CL-4B column in phosphate buffer (0.1 M, pH 7.2).

Table Ⅰ. Components of anti-EGFR immunonanoparticles containing pDNA

Components	Rationale	
Antibody; Cetuximab (Erbitux®)	It was used for targeting to EGFR in various cells and to enhance selective intracellular delivery.	
Linkage; DSPE-PEG_{2000}-MAL + Antibody	The sulfhydryl groups (SH-) in whole antibody were conjugated to liposomes and lipoplexes via a maleimide moiety for targeted binding and internalization	
DMKE	It was used for effective pDNA encapsulation or complexation with liposomes via charge interaction.	
Nanoparticles	Liposomes and virosomes	Lipoplexes and viroplexes
	Neutrally charged for *in vivo* stability	Positively charged for effective cell binding
	PEGylated for longer circulation	
	Small diameter for efficient extravasation	
Sendai viral F/HN proteins	They were inserted to increase membrane fusogenecity in virosomes and viroplexes	
Agent; Nucleic acids	A reporter gene pluc, pIL12 and pSal	

Table Ⅱ. Components of anti-EGFR immunonanoparticles (mol%)

nanoparticle	DMKE	POPC	Cholesterol	DSPE-PEG_{2000}-maleimide	DSPE-PEG_{2000}
immunoliposomes	5	91		0.2	3.8
immunovirosomes	5	91		0.2	3.8
immunolipoplexes	48		48	0.2	3.8
immunoviroplexes	48		48	0.2	3.8

6. Gel retardation and enzyme protection assay

6-1. Immunoliposomes and immunovirosomes encapsulating pDNA

To ensure antibody conjugated to immunonanoparticles, the reaction samples were analyzed by SDS-PAGE with Coomassie blue staining. The samples were tested by the enzyme protection assay using the DNase I (Sigma) (0.05 unit/ ㎍ of pDNA). Briefly, 2 ㎕ of DNase I was added the solutions of immuno liposomes and immunovirosomes with plasmid DNA (1 ㎍) and the resulting mixtures were incubated for 2 h at 37℃. The reaction was stop by addition of the stopping solution (0.5 M EDTA) and then further incubated for 45 min at room temperature. The reaction solutions were treated with 2 ㎕ of 10% Triton X-100 and incubated for additional 2 h at room temperature to release pDNA from the immunonanoparticles. Finally, the reaction mixtures were run on 1% agarose gel and pDNA bands were visualized by UV illumination. The amount of pDNA encapsulated in immunoliposomes and immunovirosomes were quantified by Quantity One Program of Gel Doc EQ system (BioRad, Hercules, USA).

6-2. Cationic immunolipoplexes and immunoviroplexes of pDNA

To ensure complete pDNA complexed with cationic immunoliposomes (immunolipoplex formation) and cationic virosomes (immunoviroplex formation), the gel retardation test was performed using agarose gel electrophoresis. A varied amount of cationic immunoliposomes was added to 1 ㎍ pDNA (N/P ratio, 1~12) and then incubated at least for 30 min. Each reaction mixture was run on 1% agarose gel and pDNA bands were visualized by UV illumination. An appropriate N/P ratio of pDNA and liposomes to complete formation of immunolipoplexes and immunoviroplexes were decided by confirming complete retardation of pDNA on the gel.

7. Analysis of vesicle size and surface charge of anti-EGFR immunonanoparticles containing pDNA

To observe the changes in size and surface charge of liposomal vesicle during pDNA encapsulation (or complexation) and antibody-coupling, the vesicular size and ζ-potential were measured using a particle analyzer. The anti-EGFR immunonanoparticle samples were diluted with a freshly filtered isotonic phosphate buffer in order to yield an appropriate counting rate (100 ㎍ lipid/㎖). All the samples were placed into the specimen holder of a Zetamaster S (Malvern Instruments Ltd., Malvern, UK) 5 min prior to measurement in order to allow equilibration under at room temperature.

8. Analysis of specific immune reactivity of Cetuximab to cancer cells

In vitro specific immune reactivity of Cetuximab was evaluated in varied cancer cell lines by using Zenon® Alexa fluor 488 (Invitrogen, Eugene, USA)-labeled Cetuximab. Briefly, 25 ㎕ of the Zenon human IgG labeling reagent (Component A) was added to 5 ㎍ of Cetuximab in 20 ㎕ PBS. After incubation for 5 min at room temperature, 25 ㎕ of the Zenon blocking reagent (Component B) was added to the reaction mixture with tapping. The antibody solution was further incubated for 5 min at room temperature and then added to SK-OV-3, A549, MCF-7 and B16BL6 cells in separate tubes (1×10^6 cells/well). The treated cells were incubated for 30 min at 4℃ under the dark condition. After washed twice with PBS, the cells were then counted by a flow cytometry analysis with FACSCaliber (Becton Dickinson, San Jose, USA).

9. *In vitro* cellular binding of anti-EGFR immunonano particles

Specific cellular binding affinities of anti-EGFR immunonanoparticles were evaluated in SK-OV-3, A549, MCF-7 and B16BL6 cells (each 4×10^4/well) with a fluorescence microscopy. The cells were grown on 13 ㎜ cover slips (Nunclon, New York, USA) in 24-well plates. Twenty four h later, the immunonanoparticles containing lissamine rhodamine B-dioleoyl phospho enthanolamine (Rho-DOPE, 0.1 mole%) were added to the A549, SK-OV-3, MCF-7 and B16BL6 cells and the treated cells were incubated for 30 min at room temperature. After washed twice with PBS, the cells on cover slips were immediately examined with a fluorescence microscope (×100).

10. Flow cytometry analysis of anti-EGFR immunonano particles containing pDNA

Specific cellular binding affinities of rhodamine-labeled anti-EGFR immunonanoparticles were also evaluated by flow cytometry. The rhodamine-labeled immunonanoparticles were added to the A549, SK-OV-3, MCF-7 and B16BL6 cells in 6-well plates (each 4×10^5/well) and then incubated for 30 min at room temperature. After trypsinized and washed with PBS, the cells were treated with 0.2% paraformaldehyde for 5 min at room temperature in dark. The cells binding to the anti-EGFR immunonanoparticles were counted by a flow cytometry analysis with a FACSCaliber (Becton Dickinson, San Jose, USA)

11. *In vitro* plasmid DNA transfection by anti-EGFR immuno nanoparticles

In vitro transfection with the anti-EGFR immunonanoparticles were performed to SK-OV-3, A549, MCF-7 and B16BL6 in 24-well plates. The four different types of anti-EGFR immunonanoparticles containing pAAVCMV-Luc (1:10 wt ratio of pDNA and lipid) prepared as described above. The prepared anti-EGFR immunonanoparticles (1 ㎍ of pDNA) were added to the cells (each 4×10^4/well). After transfection for 4 h and the treated cells were additionally incubated in fresh 10% FBS-containing media for 24 h at 37℃. The transfected cells were washed twice with PBS (pH 7.4) and lysed with 200 ㎕ of lysis buffer (1% Triton X-100, 1 mM dithiothreitol and 2 mM EDTA, pH 7.8) for 2 h at room temperature with gentle agitation. The plates were incubated at -20℃ for 20 min and thawed at room temperature. The cell lysates were centrifuged for 20 min at 4℃ and 12,000 rpm to pellet debris. Luciferase activities in the supernatant were measured with a luciferase assay kit (Promega Biosciences, San Luis Obispo, USA) and a luminometer, Minilumat LB9506 (Berthold Technologies, Bad Wildbad, Germany). The protein concentration of the supernatant was measured with the DC Protein Assay Kit (Bio-Rad, Hercules, USA). The data were expressed as relative light units (RLU) of luciferase/㎎ of total cellular proteins.

12. Competitive inhibition of anti-EGFR immunonano particles mediated *in vitro* transfection by free Cetuximab

In vitro competitive inhibition of transfection mediated by the anti-EGFR immunonanoparticles were performed in various cells cultured in 24-well plates. After incubation in the presence of free Cetuximab (1 ㎍) for 30 min, SK-OV-3, A549, MCF-7 or B16BL6 cells (each 4×10^4/well) were treated with the anti-EGFR immunonanoparticles encapsulating (or complexed with) pAAVCMV-Luc (1 ㎍). Then, the cells were transfected for 4 h and further incubated in fresh 10% FBS-containing media for 24 h at 37℃. The transfected cells were washed twice with PBS (pH 7.4) and lysed with 200 ㎕ of lysis buffer (1% Triton X-100, 1 mM dithiothreitol and 2 mM EDTA, pH 7.8) for 2 h at room temperature with gentle agitation. The cell lysates in the plates were incubated at -20℃ for 20 min and thawed at room temperature. The cell lysates were centrifuged for 20 min at 4℃ and 12,000 rpm to pellet debris. Luciferase activities in the supernatant were measured with a luciferase assay kit and a luminometer, Minilumat LB9506. The protein concentration of the supernatant was measured with the DC Protein Assay Kit. The data were expressed as relative light units (RLU) of luciferase/㎎ of total cellular proteins.

13. Cytotoxicity assay of anti-EGFR immunonanoparticles containing pDNA

Cytotoxcicity of anti-EGFR immunonanoparticles was determined by MTT assay. SK-OV-3, A549, MCF-7 and B16BL6 cells were plated into 96-well pates (each 5×10^3/well) and cultured for 24 h. The cells were treated with varied concentrations of the anti-EGFR immunonanoparticles and then cultured for 24 h. Fifty ㎕ of MTT solution (1 mg/ml) was added to the cells which were further cultured 4 h. After the media containing MTT were removed, 100 ㎕ DMSO was added to solubilize the MTT-formazan product. The absorbance at 540 nm was measured with a microplate reader (Molecular Devices, Sunnyvale, USA).

14. *In vivo* gene transfection with anti-EGFR immunonano particles containing pDNA

For *in vivo* gene delivery studies, BALB/c nude mice (BALB/cAnNcrjBfi-nu; Orient, Sungnam, Korea) were subcutaneously injected with 1×10^7 SK-OV-3 cells on the abdomen right quadrant of 4~5 weeks old. When the tumors grew to approximately 100 ㎟, the mice were injected with the prepared anti-EGFR immunonanoparticles (40 ㎍ of pAAVCMV-Luc, total volume 200 ㎕) via tail vein. Two days post injection, the tumors as well as other major organs (spleen, liver, lungs, kidneys, and heart) were excised and homogenized in a lysis buffer. The tissue lysates were centrifuged at 12,000 rpm for 20 min at 4℃ to pellet debris. Luciferase activities in the supernatants (10 ㎕) were measured with a luciferase assay kit and a luminometer as described earlier. Transfection efficiency was expressed as RLU per milligram of proteins.

15. Localization of anti-EGFR immunonanoparticles containing luciferase gene in tumor tissues

The anti-EGFR immunonanoparticles labeled with rhodamine were intravenously injected to BALB/c nude mice carrying SK-OV-3 tumors at the size of approximately 200 mm^3. The transfected tumor tissues were excised 24 h post administration. The xenografted SK-OV-3 tumors were dissected and immediately frozen. The frozen tumor tissues were transversally sectioned (3 ㎛) using a LEICA CM 1510-cryostat (LEICA, Wetzlar, Germany). The sections were examined by fluorescence microscopy (×100).

16. Immunohistochemical analysis of *in vivo* expression of anticancer genes

Anti-EGFR immunonanoparticles containing anticancer genes, pAAVCMV-mIL12 and/or pFLAG-Sal, were prepared as described above. The prepared immunonanoparticles (10 ㎍ pDNA in 200 ㎕ PBS each mouse) were intravenously administered to mice carrying SK-OV-3 tumors. The tumor tissues were excised 2 days post administration and transversally sectioned (3 ㎛) with a LEICA CM 1510-cryostat (LEICA, Wetzlar, Germany). The tumor sections were fixed in 4% paraformaldehyde solution for 6 h and stained with hematoxylin for counterstaining. The tumor sections were additionally stained with anti-FLAG antibodies (1/10, Abcam, Cambridge, UK) and anti-mouse IL12 antibodies (1/10, Abcam, Cambridge, UK) for examination of salmosin and IL12 expression, respectively. The stained tissues were then examined under a microscopy (×100).

17. *In vivo* tumor growth inhibition by administration of the anti-EGFR immunonanoparticles containing IL12 and /or salmosin genes

SK-OV-3 human ovarian cancer cells (1×10^7/mouse) were subcutaneously inoculated on the abdomen right quadrant of 4~5 week-old female BALB/c nude mice. When tumors reached a volume of approximately 50 ㎣ ([length×width^2]/2), the mice were intravenously injected with the anti-cancer gene containing anti-EGFR immunolpoplexes and immunoviroplexes (n=5) at the dose of 0.5 mg/kg (10 ㎍ of IL12 or/and salmosine, four times injection at intervals of 3 days). For co-administration of anticancer genes and chemical drugs, doxorubicin was also administered intravenously at the dose of 15 mg/kg (4 times at intervals of 3 days). Tumor growth in the treated mice was monitored for 37 days post treatment. The mice were sacrificed on day 43 and the lung colonization was counted.

Ⅲ. RESULTS

1. Preparation of four different types of anti-EGFR immuno nanoparticles containing pDNA

Conceptual illustrations of the anti-EGFR immunonanoparticles (immuno liposomes, immunovirosomes, immunolipoplexes and immunoviroplexes) are shown in Figure 1. Anti-EGFR antibody Cetuximab was conjugated to the liposomal surface by the direct coupling method. Thiolated Cetuximab antibodies were conjugated to reactive maleimide moiety of PEG termini exposed on neutral liposomes encapsulating pDNA or cationic lipoplexes. The analysis of gel filtration chromatography showed effective conjugation of the antibody molecules to the surface of liposomes and lipoplexes at 0.2:1 molar ratio of antibody and DSPE-PEG_{2000}-Mal (Figure 2).

To confirm the antibody coupling to the nanoparticle surface, the prepared immunoliposomes and immunolipoplexes were run on 12% SDS-PAGE under a reducing condition (Figure 3). The electrophoresis data also showed that antibody molecules were effectively coupled to the surface of nanoparticles.

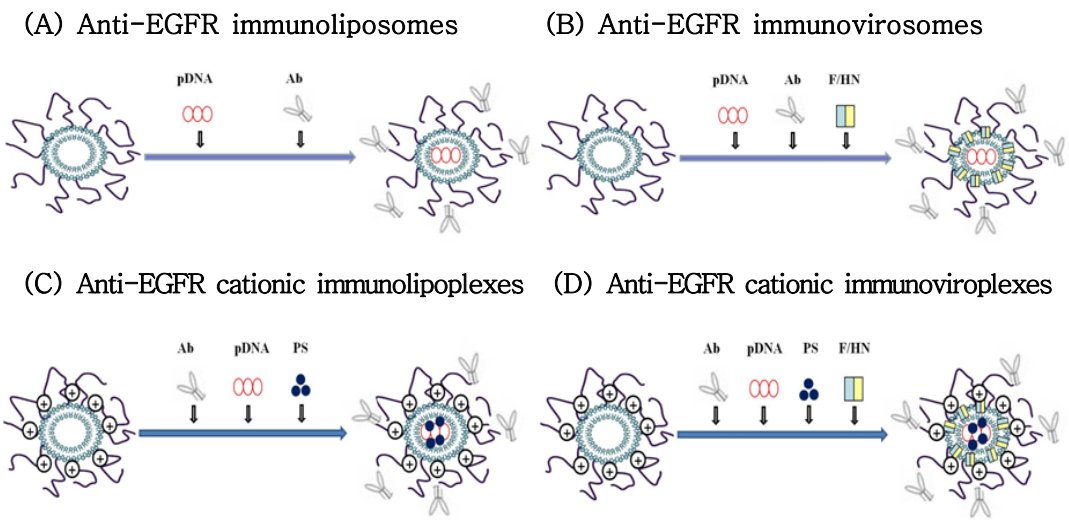

Figure 1. Schematic illustration of anti-EGFR immunonano particles.

(A) Immunoliposomes were prepared by coupling of thiolated antibodies to neutrally charged liposomes encapsulating pDNA. (B) Immunovirosomes were prepared by insertion of Sendai viral F/HN proteins into neutrally charged immunoliposomes. (C) Immunolipoplexes were prepared by coupling of thiolated antibodies to cationic liposomes and then pDNA complexation. (D) Immunoviroplexes were prepared by insertion of Sendai viral F/HN proteins into cationic lipoplexes.

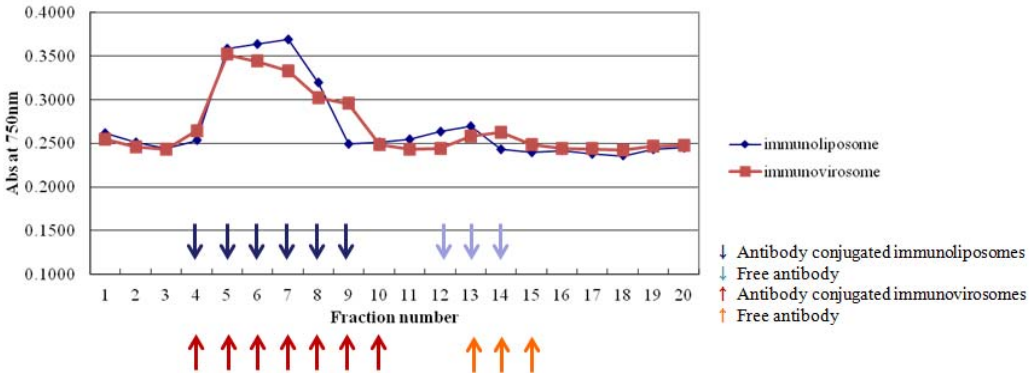

Figure 2. Elution profiles of anti-EGFR immunonanoparticles and unbound antibodies.

The reaction mixtures of nanoparticles (liposomes and virosomes) and Cetuximab antibodies were loaded onto a Sepharose CL-4B gel filtration column and eluted with 0.1 M phosphate buffer (pH 7.2). The antibody concentration of each fraction (1 ml) were quantified by protein assay.

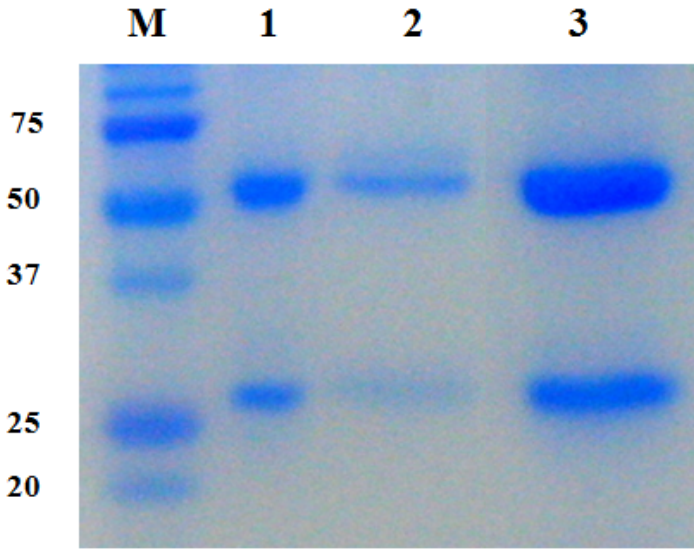

Figure 3. Analysis of antibody conjugation to immunonano partiles by SDS-PAGE.

Cetuximab antibodies were coupled to liposomal surface at 0.2:1 molar ratio of antibody and reactive maleimide and uncoupled antibodies were then removed by gel filtration. The eluted immunonanoparticles were run on 12% SDS-PAGE. M; molecular weight markers, lane 1; control Cetuximab antibody, lane 2; immunoliposomes, lane 3; immunolipoplexes.

2. Immune reactivity of Cetuximab antibody to epithelial growth factor receptor (EGFR)

Specific immune reactivity of Cetuximab antibody to EGFR over-expressed on tumor cells was examined by FACS analysis (Figure 4). Varied types of tumor cells (SK-OV-3, A549, MCF-7 and B16BL6 cells) were incubated in the presence of fluorescent Cetuximab. The Cetuximab was able to specifically bind to EGFR-expressing SK-OV-3 and A549 cells, but far less bind to MCF-7 cells. The same antibodies were not able to bind to B16BL6 cells expressing no EGFR. According to the measurement of MFI (mean fluorescence intensity), the expression levels of EGFR on the cancer cell surface were SK-OV-3>>A549>>MCF-7>B16BL6.

(A) EGFR-positive cells

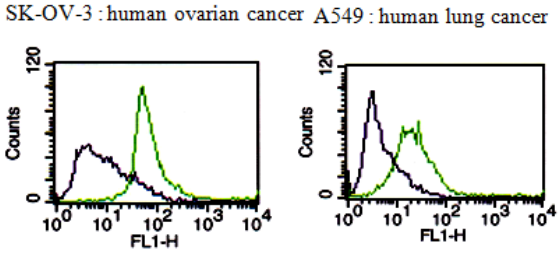

(B) EGFR-negative cells

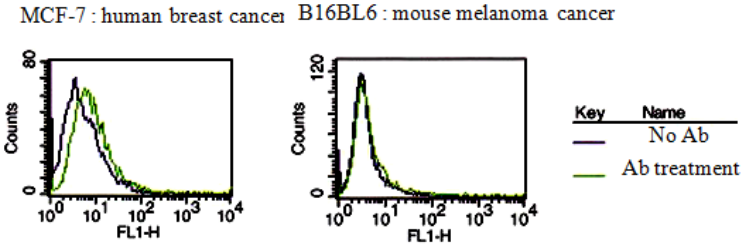

(C) MFI (mean fluorescence of intensity)

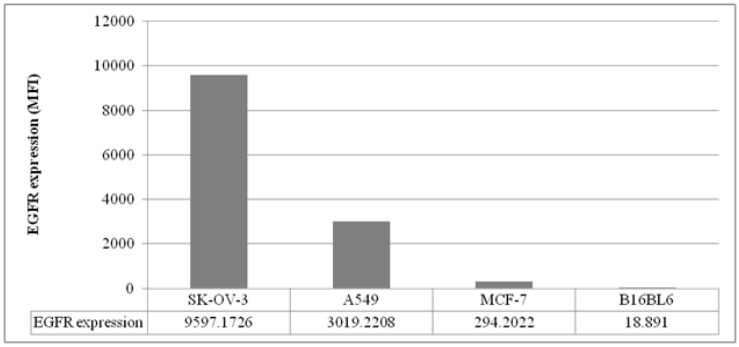

	SK-OV-3	A549	MCF-7	B16BL6
EGFR expression	9597.1726	3019.2208	294.2022	18.891

Figure 4. Specific binding of Cetuximab to EGFR-positive and EGFR-negative cancer cells.

FACS analysis was performed with EGFR-positive cancer cells (SK-OV-3 and A549) (A) and EGFR-negative cancer cells (MCF-7 and B16BL6) (B) treated with Alexa fluor 488-Cetuximab, providing their mean fluorescence of intensity (MFI) (C).

3. Preparation of anti-EGFR immunoliposomes and immuno virosomes encapsulating pDNA

For preparation of anti-EGFR PEGylated immunoliposomes and anti-EGFR PEGylated immunovirosomes, pDNA encapsulation into liposomes and virosomes is critical. After full hydration of dried lipid components with a solution containing pDNA, the resulting mixture was repeatedly frozen and thawed 10 times. To examine pDNA encapsulation, the liposome and virosome solutions were run on 1% agarose gel after treatment with DNase I and/or Triton X-100.

According to the gel retardation result (Figure 5), pDNA was efficiently encapsulated in the liposomes and virosomes. The pDNA entrapped into liposomes (Figure 5A) and virosomes (Figure 5B) did not migrate freely in the agarose gel. However, the liposomes and virosomes lysed with Triton X-100 released intact pDNA. The pDNA encapsulation efficiency was calculated from comparison of the total pDNA (lane 5) and encapsultated pDNA (lane 6) using the Quantity one program (Bio-Rad) and estimated to be approximately 70%.

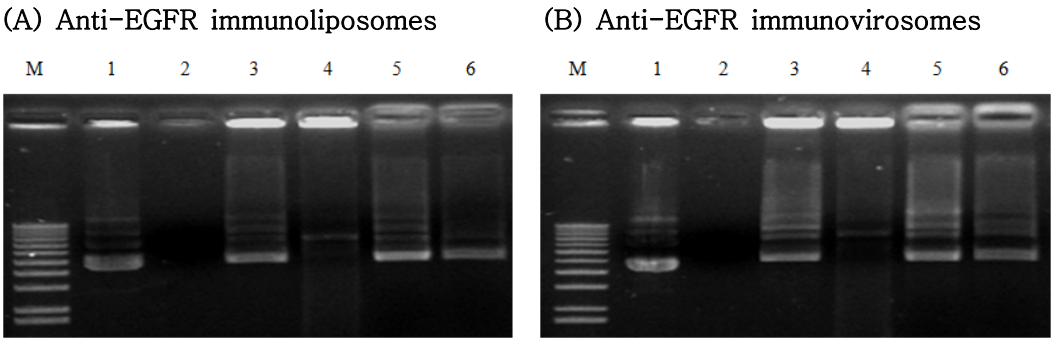

Figure 5. Encapsulation of pDNA in anti-EGFR immuno liposomes and immunovirosomes.

The anti-EGFR immunoliposomes (A) and anti-EGFR immunovirosomes (B) encapsulating pDNA were run on 1% agarose gel and visualized by UV illumination. (a) Lane M; λ/*Hin*d Ⅲ DNA molecular weight markers; lane 1, untreated naked DNA, lane 2; naked DNA treated with DNase Ⅰ, lane 3; untreated, lane 4; treated with DNase Ⅰ, lane 5; treated with Triton X-100, lane 6; treated with DNase I and then Triton X-100.

4. Preparation of cationic anti-EGFR immunolipoplexes and immunoviroplexes

Cationic lipoplexes can be defined as a complex form of cationic liposomes and negatively charged pDNA, and cationic viroplexes can be prepared by insertion of Sendai viral F/HN proteins to cationic lipoplexes. Therefore, lipoplexes and viroplexes have a different polymorphism from pDNA-encapsulating liposomes. The cationic liposomes were mixed with a buffer containing pDNA at varied charge ratios of cationic liposomes and pDNA. To verify complete pDNA complexation with liposomes, the lipoplexes prepared at 1:1 ~ 12:1 N/P ratios of cationic liposome and pDNA were run on 1% agarose gel (Figure 6). According to the gel retardation test, complete complexation of pDNA and DMKE/Chol cationic liposomes or virosomes was seen at 1:3 N/P ratio. Therefore, all lipoplexes and viroplexes utilized in this study was formulated at 1:3 N/P ratio, otherwise mentioned.

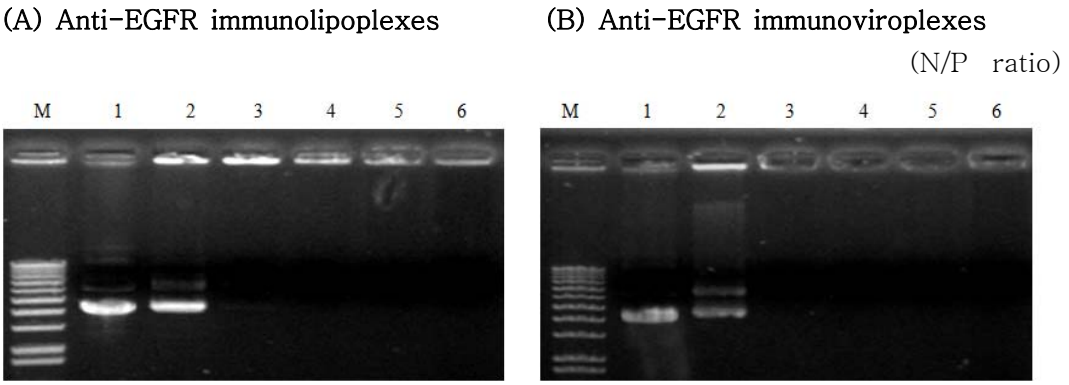

Figure 6. Complexation of pDNA with cationic anti-EGFR immunolipoplexes and immunoviroplexes.

The cationic anti-EGFR immunoliposomes (A) and virosomes (B) complexed with pDNA at varied N/P ratios were run on 1% agarose gel and visualized by UV illumination. Lane M; λ/*Hin*d Ⅲ DNA molecular weight markers, lane 1; naked DNA, lane 2-6; 1:1, 3:1, 6:1, 9:1, 12:1 N/P ratios.

5. Vesicular size and surface charge of anti-EGFR immunonanoparticles containing pDNA

The vesicular size and surface charge of anti-EGFR immunonanoparticles are major parameters *in vivo* targeting of nanoparticles to intended cells or tissues because the particle size and charge influences efficiency of the enhanced permeation and retention (EPR) effect and cellular uptake through endocytosis. According to the vesicular size measurement by a particle analyzer (Table III), generally vesicular sizes of liposomes and virosomes were slightly increased by pDNA encapsulation (or complexation), regardless of surface charge. At the same time, pDNA encapsulation reduced the surface charge of the liposomes and virosomes. Meanwhile, pDNA addition to the immunoliposomes and immunovirosomes slightly reduced their vesicular sizes as well as surface charge.

Addition of F/HN proteins to liposomal vesicles for preparation of virosomes and viroplexes increased the sizes of liposomes and lipoplexes. In addition, antibody conjugation to the liposomal surface significantly also increased vesicular sizes of the liposomes and virosomes. However, all of the finalized anti-EGFR immunonanoparticles were in an appropriate range of vesicular size smaller than 220 nm.

Table Ⅲ. Vesicular size and surface charge of anti-EGFR immunonanoparticles

Anti-EGFR immunonanoparteicles			Size (㎚)*	Zeta-potential (㎷)*
No mAb	No pDNA	Neutral liposomes	130.8 (± 3.0)**	8.2 (± 1.0)**
		cationic liposomes	98.6 (± 3.0)	56.7 (± 6.0)
		Neutral virosomes	156.3 (± 4.5)	5.8 (± 0.5)
		cationic virosomes	121.8 (± 2.3)	45.2 (± 2.7)
	with pDNA	Neutral liposomes	151.8 (± 8.9)	-3.3 (± 0.2)
		cationic lipoplexes	135.6 (± 1.0)	50.9 (± 0.3)
		Neutral virosomes	192.1 (± 2.1)	-1.9 (± 0.5)
		cationic viroplexes	136.8 (± 9.2)	38.5 (± 1.0)
with mAb	no pDNA	Anti-EGFR neutral immunoliposomes	182.8 (± 10.6)	2.1 (± 0.5)
		Anti-EGFR cationic immunoliposomes	131.3 (± 2.9)	45.4 (± 0.4)
		Anti-EGFR neutral immunovirosomes	230.7 (± 7.6)	0.5 (± 0.9)
		Anti-EGFR cationic immunovirosomes	184.6 (± 2.7)	42.1 (± 1.0)
	with pDNA	Anti-EGFR neutral immunoliposomes	173.1 (± 7.5)	-4.9 (± 0.5)
		Anti-EGFR cationic immunolipoplexes	153.1 (± 4.2)	25.4 (± 1.2)
		Anti-EGFR neutral immunovirosomes	213.5 (± 8.1)	-2.3 (± 0.4)
		Anti-EGFR cationic immunoviroplexes	179.4 (± 3.7)	21.6 (± 0.7)

* The particle size and zeta-potentials were measured 4 times using a zetasizer.

** The particles size (㎚); average particle size ± S.D.
zeta-potentials (㎷); average zeta-potentials ± S.D.

6. *In vitro* cellular binding of anti-EGFR immunonanoparticles containing pDNA

Specific cellular binding of anti-EGFR immunonanoparticles (immuno liposomes, immunovirosomes, immunolipoplexes and immunoviroplexes) labeled with rhodamine to four different cancer cells (SK-OV-3, A549, MCF-7 and B16BL6) were analysed by flow cytometery (Figure 7) and observed under a fluorescence microscope (Figure 8). As speculated, all of the anti-EGFR immunonanoparticles showed high EGFR-specific cellular binding to EGFR-positive cells (A549 and SK-OV-3 cells). Their binding affinities to EGFR-negative cell lines (MCF-7 and B16BL6 cells) were much lower than to the EGFR-positive cell lines. Meanwhile, conventional DMKE/Chol lipopolexes showed efficient binding to all types of cell regardless EGFR expression on the cell surface.

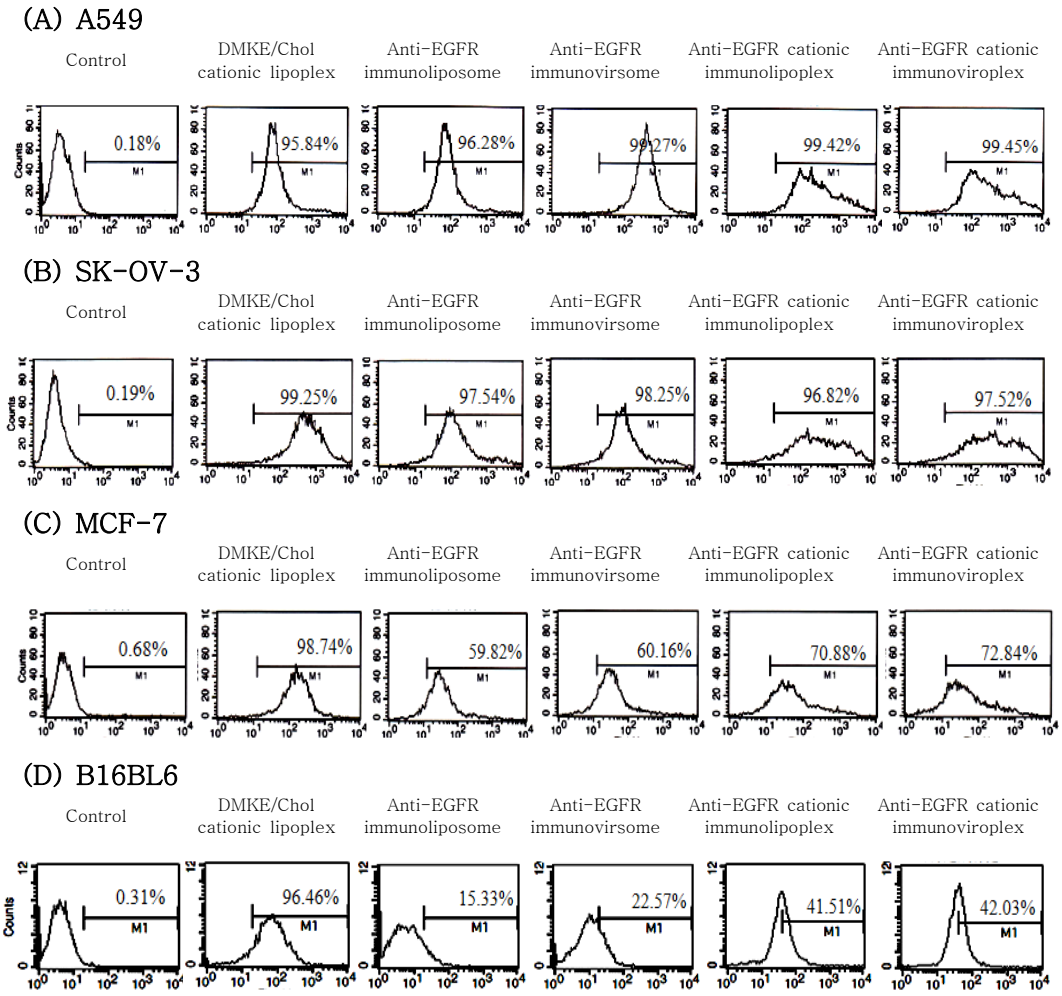

Figure 7. *In vitro* binding of the anti-EGFR immunonano particles containing pDNA to tumor cells.

The cancer cells (SK-OV-3, A549, MCF-7 and B16BL6) were incubated with rhodamine-labeled anti-EGFR immunonanoparticles for 30 min at 4℃. After washed with PBS, the cells were analysed by flow cytometry.

(A) A549

Control | Anti-EGFR immunoliposome | Anti-EGFR immunovirsome | Anti-EGFR cationic immunolipoplex | Anti-EGFR cationic immunoviroplex

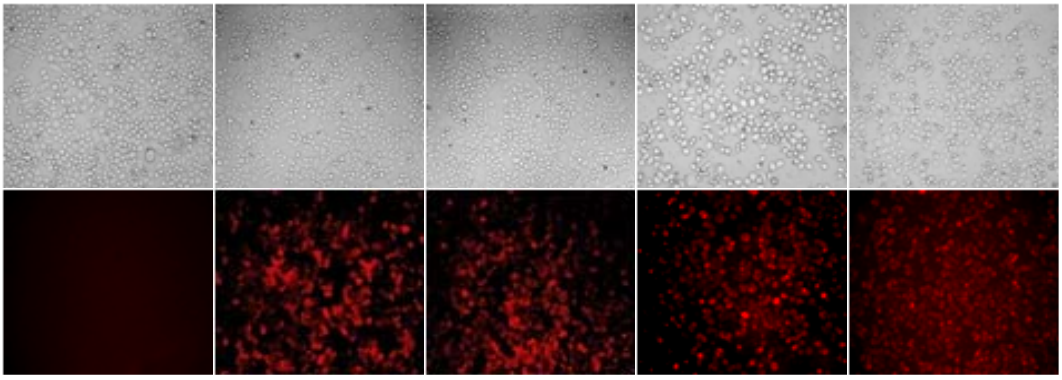

(B) SK-OV-3

Control | Anti-EGFR immunoliposome | Anti-EGFR immunovirsome | Anti-EGFR cationic immunolipoplex | Anti-EGFR cationic immunoviroplex

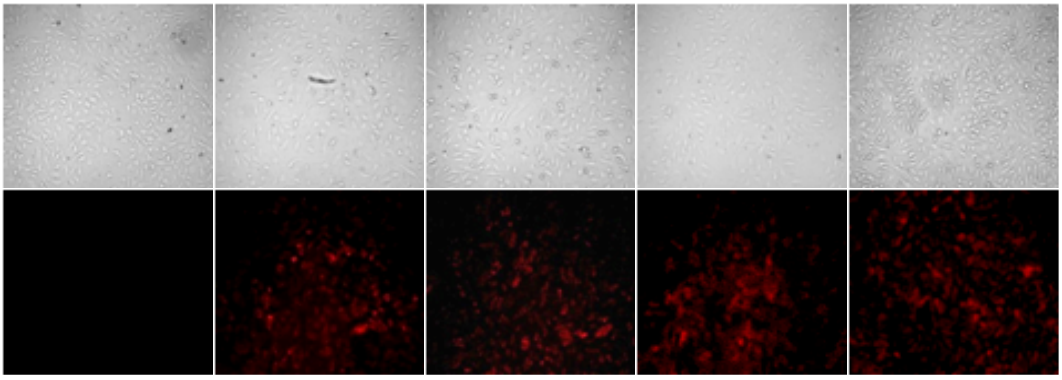

(C) MCF-7

Control | Anti-EGFR immunoliposome | Anti-EGFR immunovirsome | Anti-EGFR cationic immunolipoplex | Anti-EGFR cationic immunoviroplex

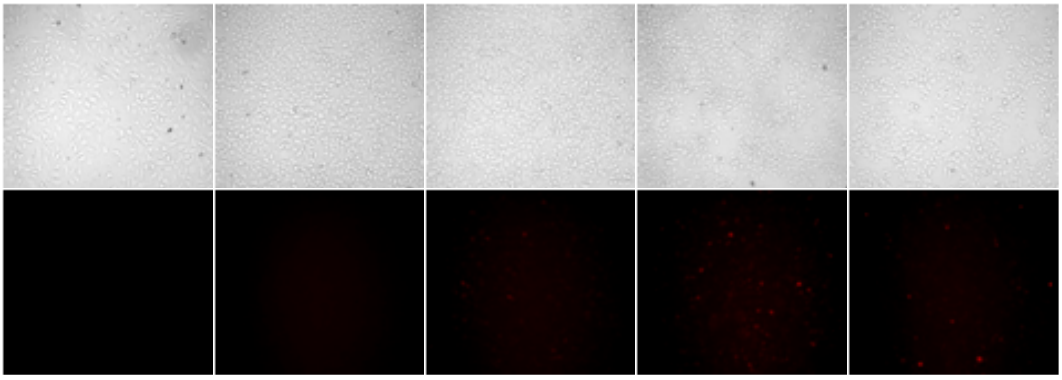

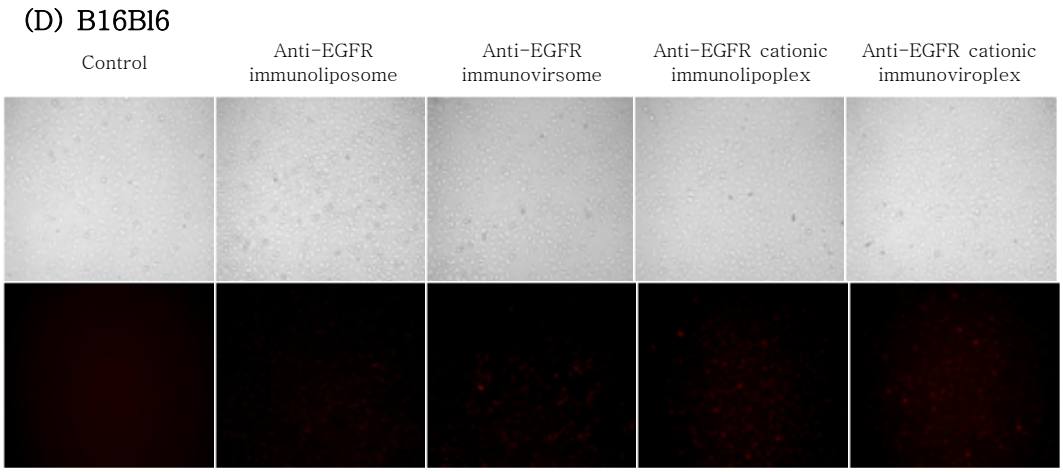

Control; non-treatment anti-EGFR immunonanoparticles

Figure 8. *In vitro* cellular binding of anti-EGFR immuno nanoparticles.

SK-OV-3 (A), A549 (B), MCF-7 (C) and B16BL6 (D) were incubated with rhodamine-labeled anti-EGFR immunonanoparticles for 30 min at 4℃. After washed with PBS, the cells were observed by fluorescence microscopy (×100). Control; untreated cells.

7. *In vitro* gene transfection by anti-EGFR immunonano particles

In vitro transfection mediated by the anti-EGFR immunonanoparticles were compared in the four different types of cancer cells; A549, SK-OV-3, MCF-7 and B16BL6 cells (Figure 9). According to the *in vitro* transfection results, the anti-EGFR immunoliposomes and immunovirosomes did not show efficient transfection and expression of luciferase in EGFR-overexpressing A549 and SK-OV-3 cells as much as the anti-EGFR immunolipoplexes and immuno viroplexes. The anti-EGFR immunolipoplexes and immunoviroplexes exhibited at least 100 folds higher transfection than the other ones under the same transfection conditions.

The levels of luciferase expression in the transfected cells were depending upon the levels of EGFR expression on the tumor cell surface. The anti-EGFR immunolipoplexes and immunoviroplexes exhibited efficient transgene expression in A549 and SK-OV-3 cells, but not in MCF-7 and B16BL6 cells. (Figure 8). Meanwhile, the conventional cationic liposomes, Lipofectamine 2000 and DMKE/Chol were able to efficiently, but nonspecifically transfect the all types of cancer cells regardless EGFR expression.

(A) A549

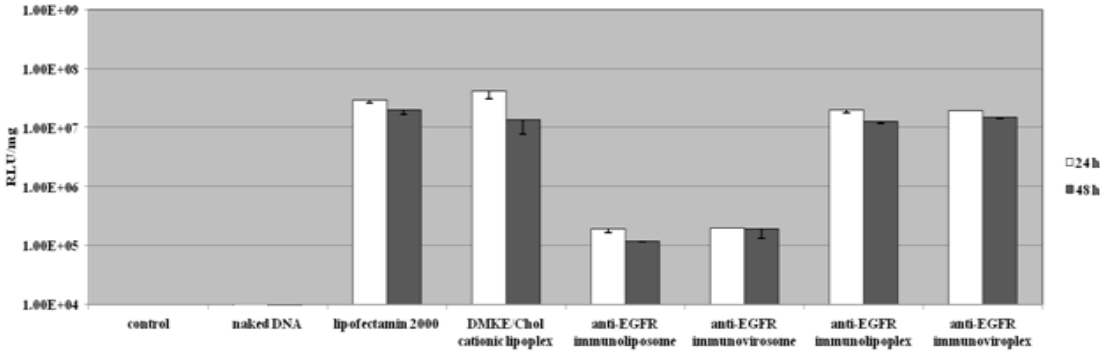

(B) SK-OV-3

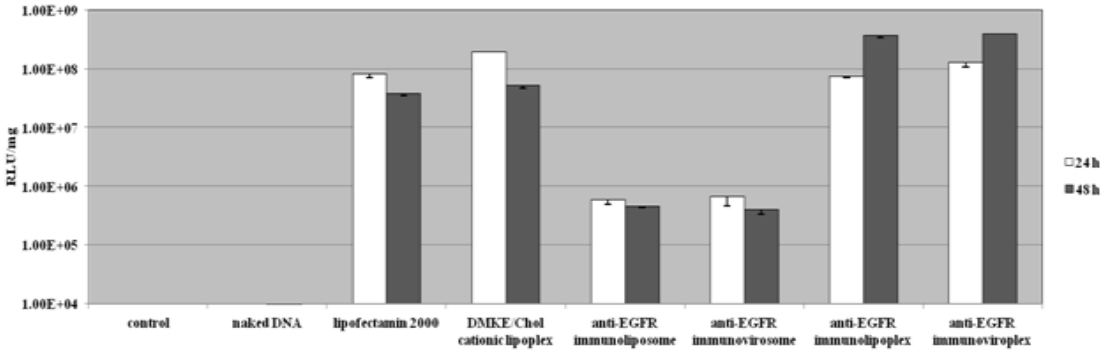

(C) MCF-7

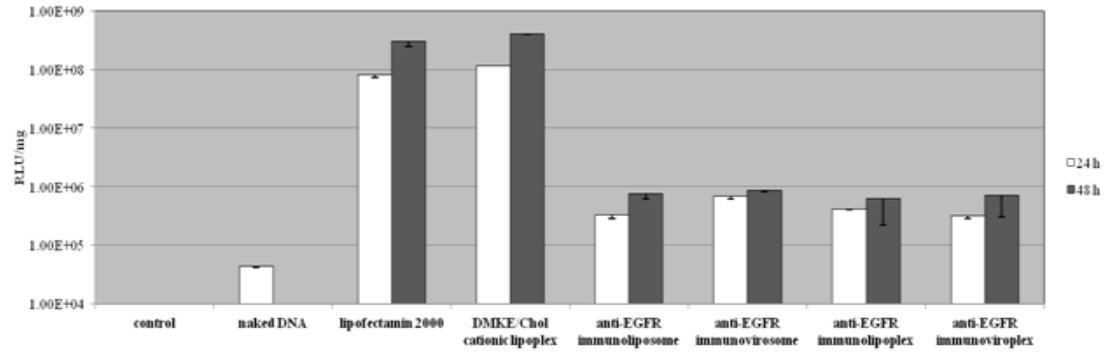

(D) B16BL6

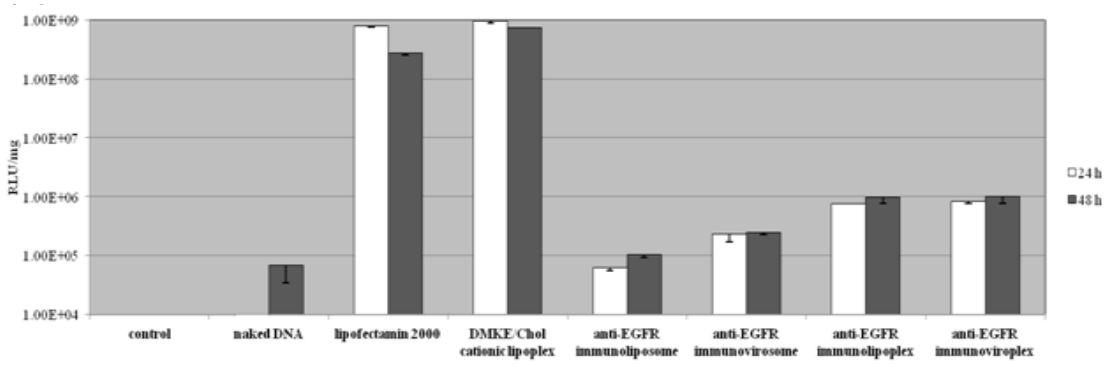

Figure 9. *In vitro* gene transfection by anti-EGFR immuno nanoparticles.

A549 (A), SK-OV-3 (B), MCF-7 (C) and B16BL6 (D) cells were transfected with the luciferase gene delivered by lipofectamine 2000, DMKE/Chol lipoplexes, and the anti-EGFR immunonanoparticles (immunoliposomes, immuno virosomes, immunolipoplexes, and immunoviroplexes). The levels of luciferase expression in the transfected cells was calculated to RLU per milligram of proteins. Each bar represents the mean ± S.D. for three separate experiments of luciferase assay.

8. Competitive inhibition of *in vitro* transfection mediated by anti-EGFR immunonanoparticles by free anti-EGFR antibodies

To verify whether efficient transfection by the anti-EGFR immunonano particles is mediated via EGF receptors, the cancer cells were pretreated with anti-EGFR antibodies (Cetuximab) before transfection. The free antibody pretreatment significantly reduced luciferase expression in SK-OV-3 and A549 (Figure 10). Meanwhile, the expression levels of luciferase in MCF-7 and B16BL6 cells were little affected by pretreatment with the free antibodies. This result also shows that the anti-EGFR antibodies coupled to the surface of nanoparticles is a critical ligand to mediate transfection to cancer cells overexpressing EGFR.

(A) A549

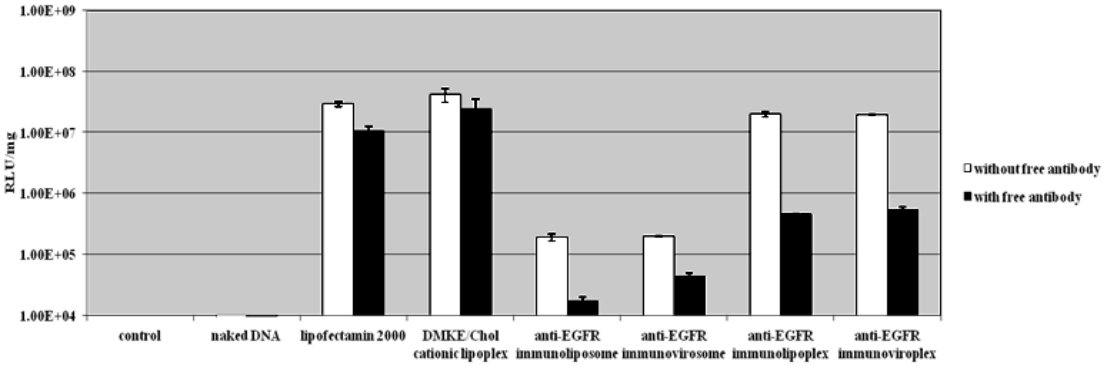

(B) SK-OV-3

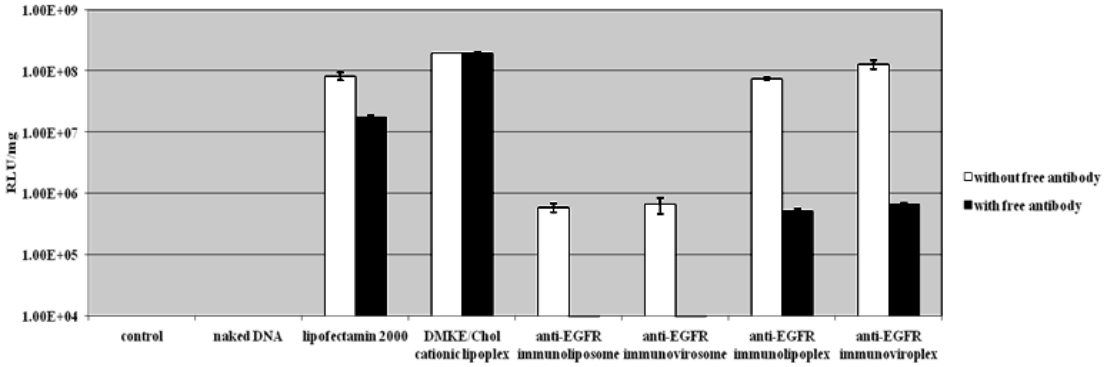

(C) MCF-7

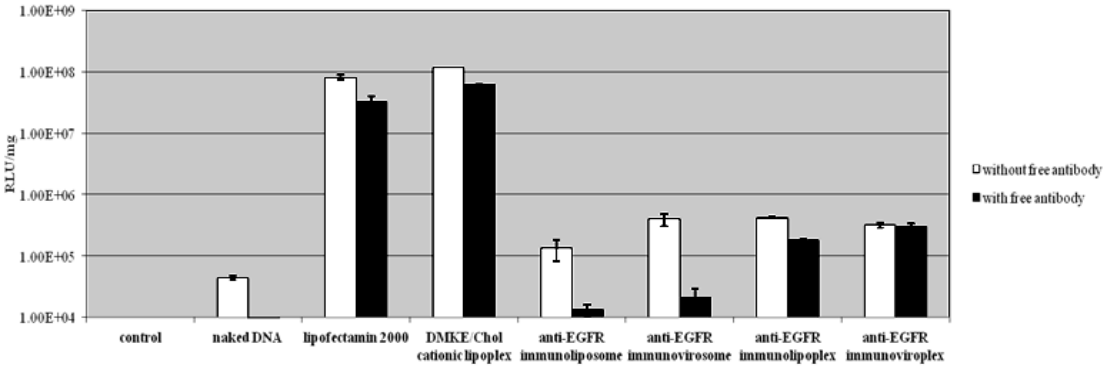

(D) B16BL6

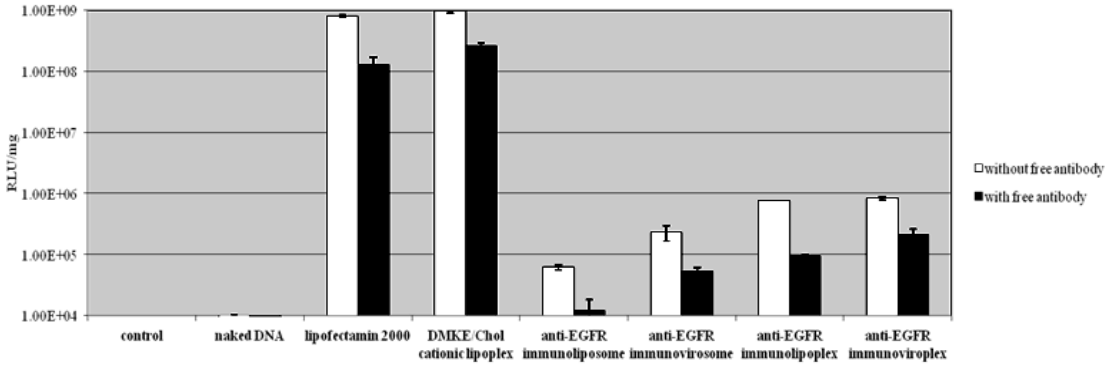

Figure 10. Competitive inhibition of *in vitro* transfection mediated by anti-EGFR immunonanoparticles by free Cetuximab.

A549 (A), SK-OV-3 (B), MCF-7 (C) and B16BL6 (D) cells were pretreated with free Cetuximab antibodies and then transfected with the anti-EGFR immunonanoparticles. Luciferase expression in the cells was calculated to RLU per milligram of proteins. Each bar represents the mean ± S.D. for three separate experiments of luciferase assay.

9. *In vitro* cytotoxicity of anti-EGFR immunonanoparticles

The varied amounts of anti-EGFR immunonanoparticles were treated to A549, SK-OV-3, MCF-7 and B16BL6 cells to measure their cell toxicity (Figure 11). Generally, the anti-EGFR immunonanoparticles were less cytotoxic to the all types of cells tested than the cationic DMKE/Chol lipoplexes. At the ranges of nanoparticles concentration for *in vitro* and *in vivo* transfection (1 ~ 50 ㎍/㎖), the anti-EGFR immunonanoparticles did not severely damage the four different cultured cells, exhibiting over 80% cell viability. Among the anti-EGFR immunonanoparticles, the anti-EGFR immunolipoplexes and immunoviroplexes appeared to be more toxic than the other ones. MCF-7 cells was more sensitive to the anti-EGFR immunonanoparticles than other cell lines, resulting in less survival under the same transfection conditions.

(A) A549

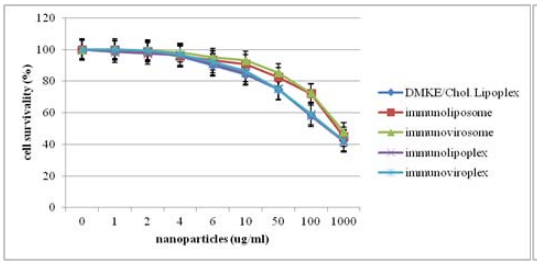

(B) SK-OV-3

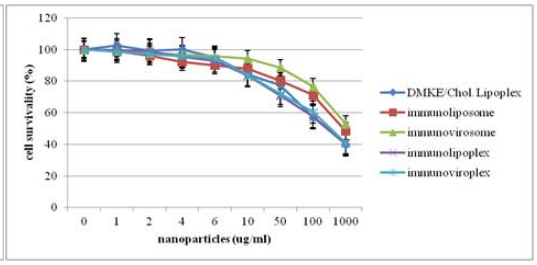

(C) MCF-7

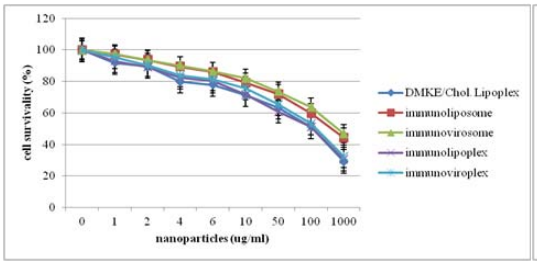

(D) B16BL6

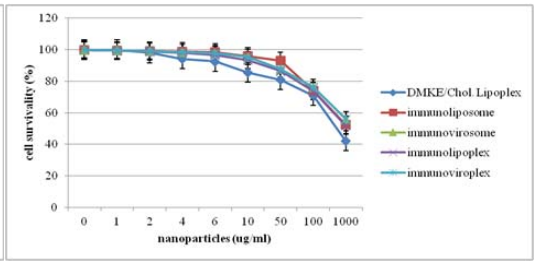

Figure 11. *In vitro* cytotoxicity of anti-EGFR immunonano particles.

A549 (A), SK-OV-3 (B), MCF-7 (C) and B16Bl6 (D) cells were treated with the various concentrations of anti-EGFR immunonanoparticles (immunoliposomes, immunovirosomes, immunolipoplexes and immunoviroplexes) and then cultured for 24 h. Cell viability was measured by the MTT assay.

10. *In vivo* gene transfection mediated by anti-EGFR immunonanoparticles

To investigate tumor targeting capabilities and biodistribution patterns of anti-EGFR immunonanoparticles (immunoliposomes, immunovirosomes, immuno lipoplexes and immunoviroplexes) were intravenously injected to BALB/c nude mice carrying SK-OV-3 tumors. The levels of luciferase expression in collected internal organs (spleen, liver, lungs, kidneys, heart and tumor) was compared to each other (Figure 12). The anti-EGFR immunonanoparticles exhibited 10~250 fold higher gene expression in tumor than the DMKE/Chol cationic lipoplexes. Among the EGFR-directed nanoparticles, the anti-EGFR immunolipoplexes and immunoviroplexes were more efficient than the other gene delivery systems. However, regardless the types of nanoparticle formulation, they still showed relatively high nonspecific transfection to the lungs and liver. Nevertheless, the anti-EGFR immunoviroplexes showed the highest transfection in the SK-OV-3 tumors overexpressing EGFR. This implies that the efficient *in vivo* transfection by the anti-EGFR immunoviroplexes may be due to tumor-recognizing ligands (Cetuximab) coupled to the surface of nanoparticles and fusogenic F/HN viral proteins reconstituted in the membrane vesicles.

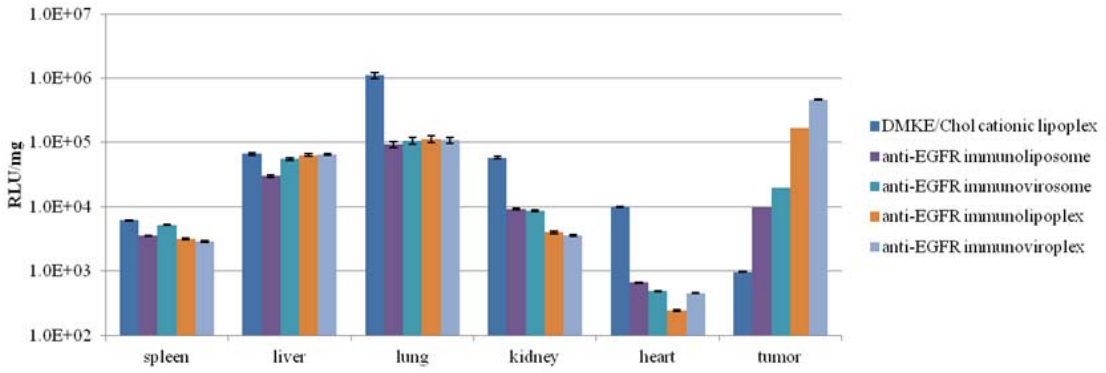

Figure 12. *In vivo* gene transfection mediated by anti-EGFR immunonanoparticles.

A tumor-xenografted mouse model was prepared by subcutaneous inoculation of SK-OV-3 cells to BALB/c nude mice. The anti-EGFR immuno nanoparticles containing 40 ㎍ pDNA encoding luciferase gene were intravenously administered to the mice carry tumors (tumor volume ~200 ㎣). The mice were sacrified 24 hours post injection and major organs were collected. The luciferase expression in the spleen, liver, lungs, kidneys, heart and tumor tissues were assayed and calculated to RLU per milligram of proteins. Each bar represents the meas ± S.D. for three separate experiments of luciferase assay.

11. Tumor localization of anti-EGFR immunonanoparticles containing pDNA intravenously administered

For histological analysis of rhoamine-labeled DMKE/Chol cationic lipoplexes and anti-EGFR immunonanoparteicles (immunoliposomes, immunovirosomes, immunolipoplexes and immunoviroplexes) were intravenously injected to BALB/c nude mice carrying SK-OV-3 tumors. Then, the dissected tumor tissues were examined by fluorescence microscopy (Figure 13). All of the anti-EGFR immunonanoparticles intravenously administered were specifically localized in the tumor tissues. Among the anti-EGFR immunonanoparticles, the anti-EGFR immunolipoplexes and anti-EGFR immunoviroplexes showed more effective localization in the tumors than the other ones. Meanwhile, the conventional DMKE/Chol cationic lipoplexes were little found in the tumors under the same transfection conditions.

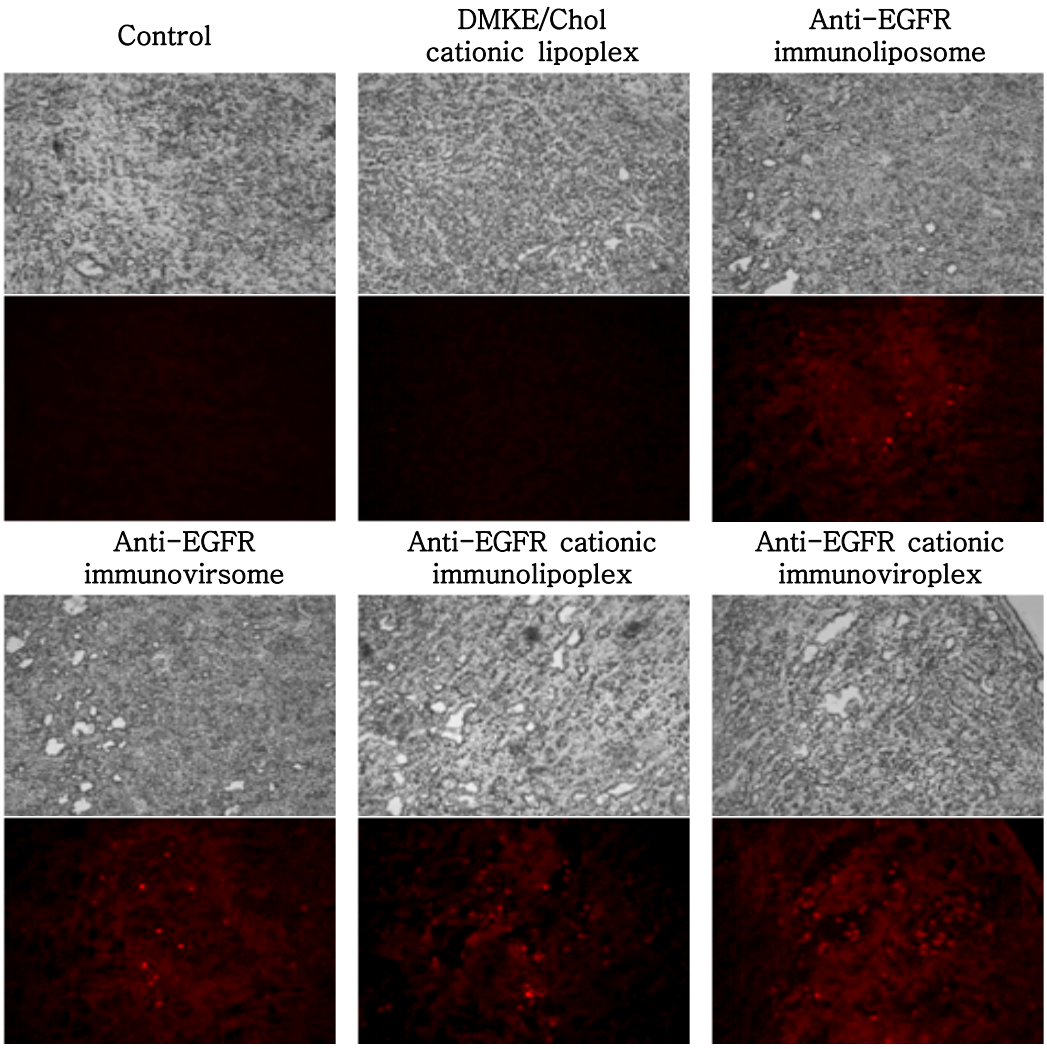

Figure 13. Localization of anti-EGFR immunonanoparticles in tumor tissues.

Rhodamine-labeled cationic lipoplexes and anti-EGFR immunonanoparticles were intravenously administered to SK-OV-3-xenografted nude mice (tumor volume, ~100 ㎣). After 24 h post injection, anti-EGFR immunonanoparticles localized in tumor cells were observed under a fluorescence microscope (×100).

12. *In vivo* gene expressing by systemic administration of anti-EGFR immunonanoparticles with anti-cancer genes

To verify the *in vivo* gene transfection capability of the anti-EGFR immunonanoparticles, they were administered intravenously to SK-OV-3-xenografted mice via the tail vain. The anti-EGFR immunonanoparticles with 10 ㎍ of pIL12 or 10 ㎍ of pSal were injected into each mouse. The tumor sections were immunostained using anti-IL12 and anti-FLAG antibody and then examined by fluorescence microscopy. The anti-EGFR immunonano particles were relatively more effective in expression of IL12 and salmosin proteins in the tumor tissues than the conventional DMKE/Chol cationic lipoplexes (Figure 14). Among the anti-EGFR immunonanoparticles tested, the anti-EGFR immunolipoplexes and anti-EGFR immunoviroplexes showed better transgene expression in the tumors.

(A) pIL12

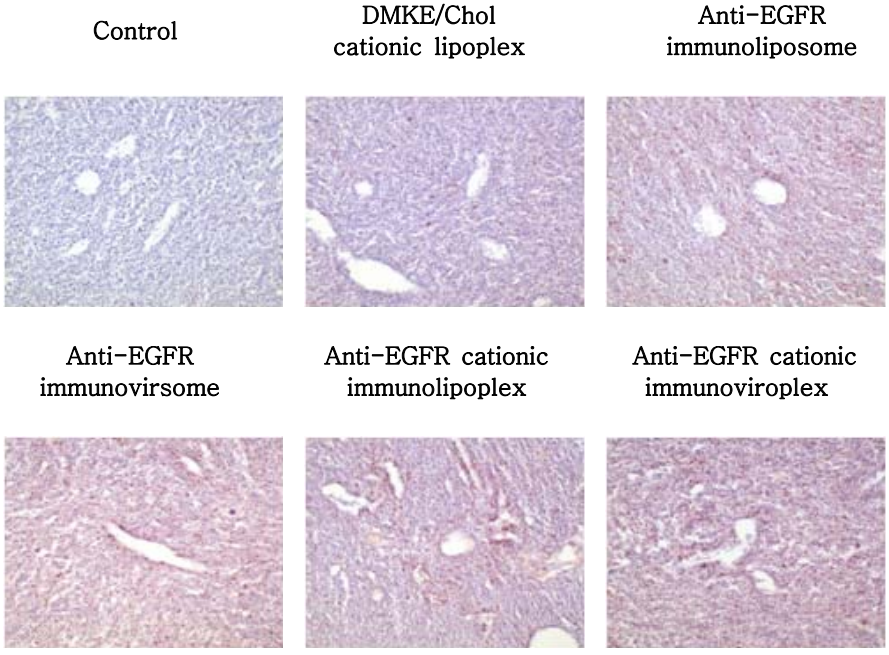

(B) pSalmosin

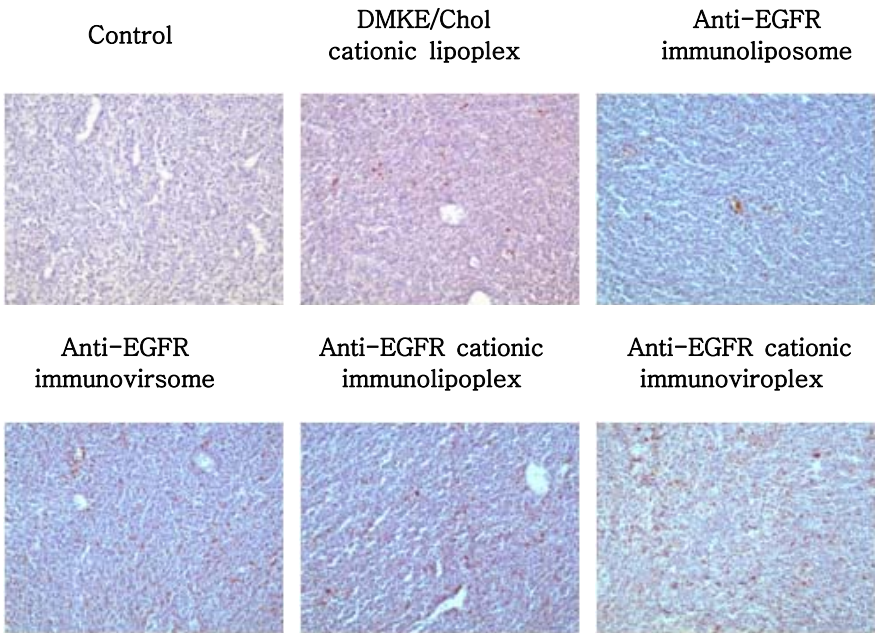

Figure 14. *In vivo* expression of IL12 and salmosin proteins mediated by anti-EGFR immunonanoparticles.

The anti-EGFR immunonanoparticles containing anti-cancer genes (pIL12 or pSal) were intravenously administered to SK-OV-3-xenografted nude mice. The tumor tissues were dissected 24 h post injection. The tumor sections were immunostained and observed under a microscope (×100).

13. Inhibition of SK-OV-3 tumor growth by administration of anti-EGFR immunonanoparticles containing IL12 or/and salmosin genes

Mice carrying SK-OV-3 tumors were prepared as described above. Since the anti-EGFR immunolipoplexes and -immunoviroplexes were more effective in *in vivo* transgene expression, only these two formulations containing IL12 or/and salmosin genes were prepared and then intravenously injected to the mice carrying tumors four times at intervals of 3 days. During 37 days of observation, significant inhibition of tumor growth was seen in all treated mice with the tendency to tumor inhibition becoming apparent with days (Figure 15). Co-treatment of pIL12 and pSalmosin were able to inhibited tumor growth more effectively than administration of either gene alone. In addition, the anti-EGFR antibody-conjugated immunolipoplexes and immunoviroplexes were clearly more effective in inhibition of tumor growth than the lipoplexes and viroplexes without anti-EGFR antibodies (Figure 16).

When the mice were treated with the anti-EGFR immunolipoplexes (or immunoviroplexes) containing pIL12/pSal and doxorubicin together, their effects on tumor growth were synergistic (Figure 17). Compared with the untreated one, co-administration of the anti-EGFR immunolipoplexes (or immunoviroplexes) containing pIL12/pSal was able to inhibit the tumor growth by 45 ~ 57% by day 37 post tumor inoculation. However, combined treatment with doxorubicin and the anti-EGFR immunolipoplexes (or immunoviroplexes) containing pIL12/pSal further inhibited the tumor growth by 80~84% reduction), compared with the treatment with the anti-EGFR immunolipoplexes (or immunoviroplexes) alone.

On day 37 post tumor injection, the all mice were sacrificed and the number of metastased colony in the lungs were counted (Figure 17). The pattern of metastasis inhibition by the anti-EGFR immunonanoparticles containing pIL12 and/or pSal was similar to that of tumor growth inhibition by the same treatment. Co-administration of the two genes was more effective in inhibition of pulmonary metastasis than treatment with either gene alone. Also, the anti-EGFR immunolipoplexes and immunoviroplexes showed more effective

inhibition of metastasis than lipoplexes and viroplexes with no anti-EGFR antibodies. Additional treatment with doxorubicin also showed a synergstic effect on inhibition of metastasis in the lungs.

(A) Tumor volume

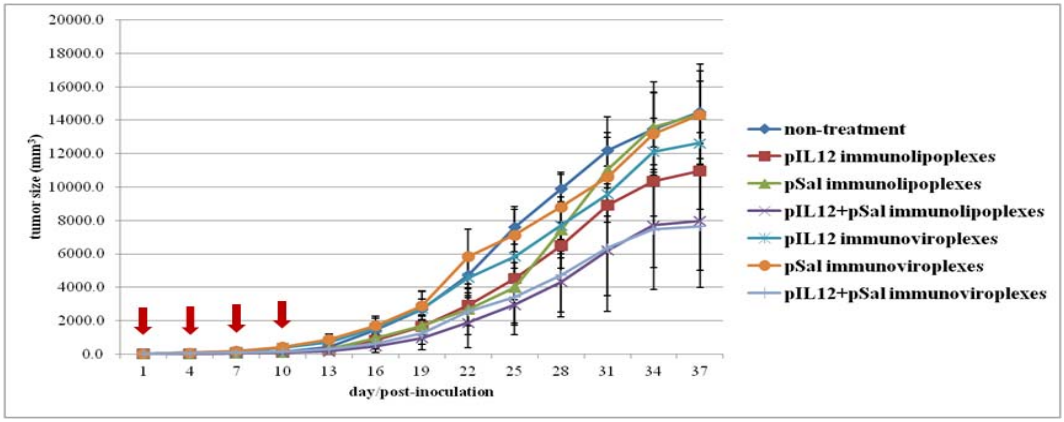

(B) Counting of lung tumor colony

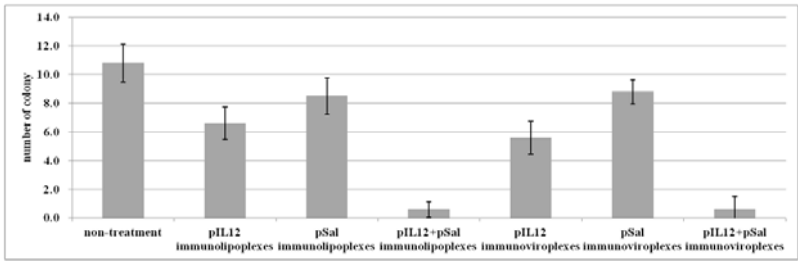

Figure 15. Tumor growth inhibition by administration of anti-EGFR immunonanoparticles containing IL12 and salmosin genes.

The varied anti-EGFR immunonanoparticles containing pIL12 and/or pSal (0.5 mg/kg) were intravenously administered to mice carrying SK-OV-3 tumors. The tumor growth was measured for 37 days (A) and whereafter colony numbers in the lungs were counted (B). Solid arrows indicate the administrations of the anti-EGFR immunonanoparticles.

(A) Tumor volume

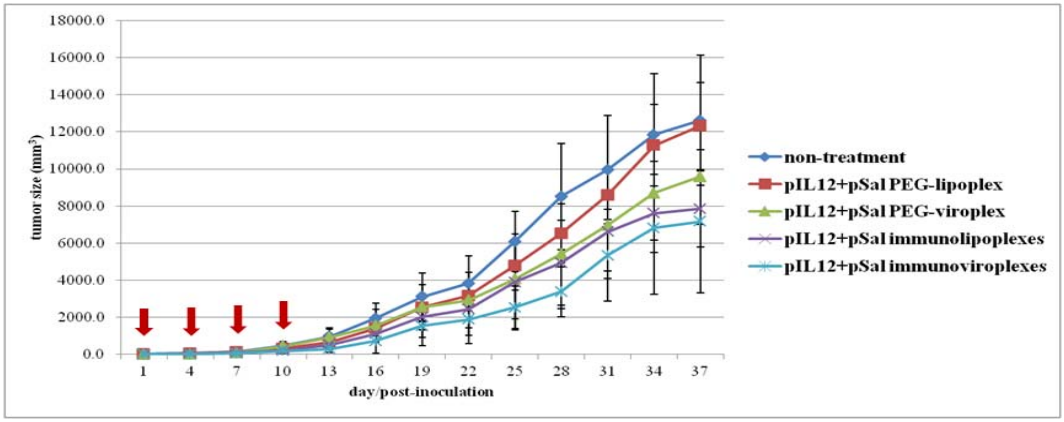

(B) Counting of lung tumor colony

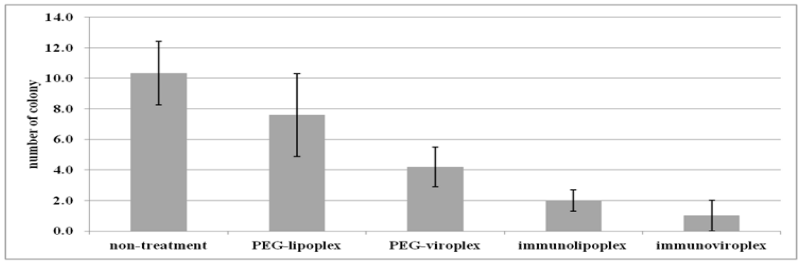

Figure 16. Tumor growth inhibition by administration of anti-EGFR immunonanoparticles containing pIL12/pSal and nanoparticles without anti-EGFR antibodies containing pIL12/pSal.

The varied anti-EGFR immunonanoparticles containing pIL12 and/or pSal or nanoparticles with no anti-EGFR antibodies containing pIL12 and/or pSal (0.5 mg/kg) were intravenously administered to mice carrying SK-OV-3 tumors. The tumor growth was measured for 37 days (A) and whereafter colony numbers in the lungs were counted (B). Solid arrows indicate the administrations of the anti-EGFR immunonanoparticles.

(A) Tumor volume

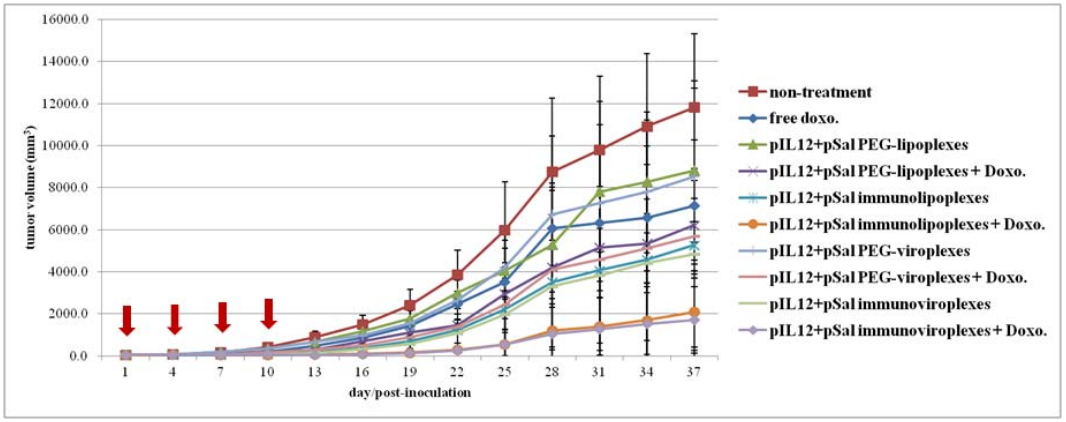

(B) Counting of lung tumor colony

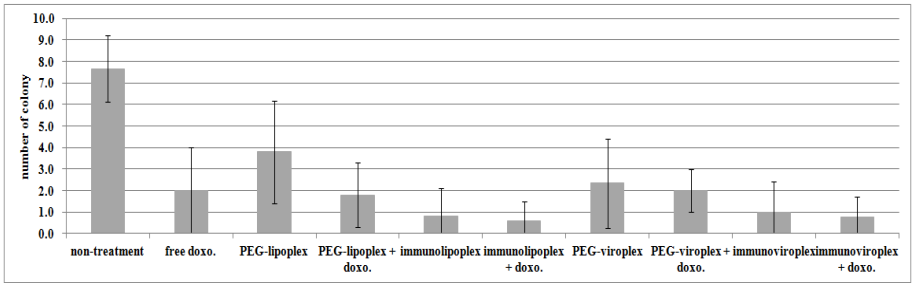

Figure 17. Tumor growth inhibition by co-administration of anti-EGFR immunonanoparticles containing pIL12/pSal and doxorubicin.

The varied anti-EGFR immunonanoparticles containing pIL12 and/or pSal (0.5 mg/kg) and doxorubicin (15 mg/kg) were intravenously administered to mice carrying SK-OV-3 tumors. The tumor growth was measured for 37 days (A) and whereafter colony numbers in the lungs were counted (B). Solid arrows indicate the administrations of the anti-EGFR immunonanoparticles.

Ⅳ. Discussion

A variety of gene delivery systems including viral vectors and nonviral vectors have been adopted in gene therapy. It has been considered that the viral vectors are a more effective gene delivery system than nonviral vectors. However, they are more immunogenic, cytopathic, and sometimes carcinogenic (44). In contrary, the nonviral vectors are safely adaptable gene delivery systems. Among them, liposomal systems are easy to be formulated by simple mixing of cationic liposomes and anionic nucleic acids (45). A number of cationic liposomes have been developed and tested in various *in vitro* and *in vivo* models (46). However, it has been considered that the liposomal vectors are not efficient in *in vivo* transfection as much as viral vectors. Therefore, a number of groups have spent a great deal of efforts to enhance their *in vivo* transfection capabilities in many ways. One of the efforts is development of virosomes prepared by reconstitution of fusogenic viral envelope proteins into liposomes to improve gene internalization into cytoplasm (47). Another effort was conjugating cell-targeting ligands to the liposomal systems to provide target-specificity. The transfection efficiency of liposomal vectors was dramatically increased when they bear a ligand recognized by a cell surface receptor (48-52).

This study aimed to focus on the issue of developments of target-specific gene delivery systems of liposomal nanoparticles. Next, two different types of anticancer genes were formulated with the target-specific liposomal nanoparticles and then delivered to a animal model carrying tumors to verify their gene-transferring capabilities. At the same time, anti-tumoral activity of the transgenes delivered by the tumor-directed gene delivery systems was also evaluated in the animal model.

First of all, four different types of liposomal nanoparticles (liposomes, virosomes, lipoplexes and viroplexes) containing pDNA molecules inside were prepared. Liposomes and virosomes are encapsulating pDNA, and lipoplexes and viroplexes are complexed with pDNA and cationic liposomes via charge interactions. The all liposomal nanoparticles were PEGylated (4 mol%) to prolong their *in vivo* circulation longevity, presumably resulting in enhanced

extravasation across the leaky endothelium of solid tumors (53). Therefore, tumor-directed anti-EGFR antibodies (Cetuximab) were coupled to PEG termini on the surface of liposomal nanoparticles for the same purposes. The anti-EGFR immunonanoparticles were prepared stably small, measured below 200 ㎚ diameter. Their sizes were small enough to extravasate through loose blood vessels and exhibit enhanced permeation and retention (EPR) effect in solid tumors.

The prepared four different types of anti-EGFR immunonanoparticles (immunolipsomes, immunovirosomes, immunolipoplexes and immunoviroplexes) were tested in various cancer cells (A549, SK-OV-3, MCF-7 and B16BL6) in terms of cell binding and gene transfection. All of the systems exhibited efficient cellular binding to EGFR-positive cells (A549 and SK-OV-3 cells), but not to EGFR-negative cells (MCF-7 and B16Bl6 cells). This result suggested that the newly developed systems would be a good gene transfection system for cancer cells overexpressing EGFR.

However, transfection efficiencies of the anti-EGFR immunonanoparticles were different depending upon the types of formulations. As expected, the all anti-EGFR immunonanoparticles showed a low level of gene transfection to the EGFR-negative cell line (MCF-7 and B16BL6 cells). Meanwhile, the anti-EGFR immunolipoplexes and immunoviroplexes were effective in *in vitro* transfection to A549 and SK-OV-3 cells, but the other two types were less effective under the same transfection conditions. The competitive inhibition of transgene expression by pretreatment of Cetuximab suggested that the effective gene expression by the immunolipoplexes and immunoviroplexes was mediated by recognition of Cetuximab by the EGF receptors on the surface of cancer cells followed by endocytosis. These results suggest that the anti-EGFR immunolipoplexes and immunoviroplexes are a better EGFR-directed gene delivery system than the others. Among them, the anti-EGFR immunoviroplexes was the best transfecton system for cancer cells expressing EGFR.

The same conclusion was drawn from the *in vivo* gene transfection experiment. The anti-EGFR immunolipoplexes and immunoviroplexes were shown higher gene expression in SK-OV-3 tumor tissues than the other ones. Especially, the anti-EGFR immunoviroplexes showed the highest gene

expression in the tumor mass. This data implied that PEGylation of the cationic complex types of immunonanoparticles were able to effectively evade serum proteins, resulting in less taken-up by phagocytes and the RES. At the same time, the cationic surface charges of the anti-EGFR immunolipoplexes and immunoviroplexes might help intracellular translocation of cargo genes via endocytosis.

Therefore, only the anti-EGFR immunolipoplexes and immunoviroplexes containing anticancer IL12 and/or salmosin genes were prepared and then intravenously injected to mice carrying SK-OV-3 tumors for anticancer gene therapy. In another set of *in vivo* experiment, the mice carrying tumors were intravenously transfected with pIL12 and/or pSal were also cotreated with an anti-cancer drug, doxorubicin. According to the experimental results, co-transfection of IL 12 and salmosin genes was able to synergistically inhibit *in vivo* tumor growth and metastasis of SK-OV-3. Another synergistic inhibition of tumor progression was shown by the combined treatment with genes and an anticancer chemical drug. The inhibition of tumor growth and metastasis by the anti-EGFR immunonanoparticles of pIL12 and salmosin genes was further enhanced by doxorubicin treatment. These data imply that varied concepts of anticancer medicine with different anticancer mechanisms can be combined to elicit a better outcome of cancer treatment regardless of whether gene medicines or chemical drugs. These *in vivo* data also verified that the anti-EGFR immunoviroplexes are the most effective EGFR-directed gene delivery system for *in vitro* and *in vivo* transfection of anticancer genes to tumor cells expressing EGFR.

A major difference between liposomes (or virosomes) and lipoplexes (or viroplexes) was a surface charge on the vesicles. The immunolipsomes and immunovirosomes had -2.3 mV and -4.9 mV of surface charge, respectively. Meanwhile, the immunolipoplexes and immunoviroplexes showed a relatively higher 25.4 mV and 21.6 mV, respectively. This difference may affect the polymorphism of immunoparticles. The liposome types had to encapsulate pDNA inside vesicle in a less efficient way. Meanwhile, it was easy for the lipoplex types to be formed resulting from charge interactions between anionic pDNA and cationic liposomes.

The differences in charge and particle polymorphism affected their

transfection processes *in vitro* and *in vivo*. Although the cells were treated with the same amount of pDNA (1 ㎍/well), the anti-EGFR immunolipoplexes and immunoviroplexes were more effective in transfection to EGFR-expressing tumor cells *in vitro* and *in vivo*. Some extents of surplus cationicity on the immunonanoparticles may help interactions between vesicle membranes and plasma membranes.

In conclusion, the anti-EGFR immunonanoparticles were able to specifically recognize the tumor cells overexpressing EGFR. Among the immunonanoparticles, the anti-EGFR immunoviroplexes were the most efficient EGFR-directed transfection systems. Anticancer IL12 and salmosin genes transferred by the immunoviroplexes were able to most efficiently inhibit EGFR-expressing tumors xenografted in mice. This system would be applicable to cancer gene therapy as an efficient tumor-directed gene carrier system.

PART Ⅱ

Tumor-directed small interfering RNA delivery by anti-EGFR immunonanopaticles

1. INTRODUCTION

RNA interference (RNAi) gained world-wide attention in 1998 because of its pivotal role in gene expression (54). RNAi is a mechanism for RNA-guided regulation of gene expression in which double-stranded RNA inhibits the expression of genes with complementary nucleotide sequences. This is a general and fundamental pathway in eukaryotic cells by which target sequence-specific small interfering RNA (siRNA) is able to target and cleave complementary mRNA (55).

In recent years, gene therapy using small interfering RNA represents as a potent and specific method in the field of targeted gene therapy (56, 57). A number of siRNA molecules have been suggested as a functional mediator of RNAi that could achieve sequence-specific gene knockdown in cancer cells. Although siRNA has the potential to be a powerful therapeutic gene as a drug, it has to be delivered inside cells effectively in order to exhibit its biological activity. Therefore, an increasing number of biotechnological and pharmaceutical companies are attempting to develop RNAi-based drugs for prevention and treatment of human diseases such as genetic diseases, infectious diseases and cancers, etc.

Target-specific siRNA delivery systems have been always a primary concern in the field of clinical applications of siRNAs (58, 59). Therefore, the major challenge for siRNA applications has been development of an efficient siRNA systemic delivery system (60, 61). Although there is still much to be improved, liposomal vector-based delivery systems have been successfully utilized in the systemic delivery of siRNAs (61). For example, Li et al. developed a LPD (liposome-polycation-DNA complex) system coupled with ligands for a sigma receptor and then showed effective delivery of siRNAs to tumor cells overexpressing sigma receptors (62, 63). In addition, a number of research groups has adopted tumor-directed antibodies as targeting ligands for tumors. Varied monoclonal antibodies (mAbs) or mAb fragments against specific tumor antigens were the most frequently ligands for tumor-targeted delivery of siRNA (64).

Antibodies as a targeting ligand for liposomal vectors have many

advantages. Firstly, antibodis have higher specificity and affinity than the small molecule ligands such as synthetic peptides. Secondly, antibody molecules provide easily accessible conjugation sites (carboxyl and thiol groups) for crosslinking of liposomal vectors (65). Thirdly, many monclonal antiibodis have been approved by US FDA (Food and Drug Administration) for cancer therapy, while other ligands such as RGD peptides are not approved yet. Among the clinically approved antibodies, Cetuximab, the anti-EGFR (epidermal growth factor receptor) mAbs or its derivatives are widely used for target-specific gene delivery of liposomal vectors to EGFR-overexpressing cancer cells (66, 67).

EGFR is a 170 kDa glycoprotein consisting of an extracellular ligand-binding domain, a transmembrane anchoring domain and an intracellular multifunctional tails (68, 69). Also, it is known to be related to cell migration, proliferation, and differentiation. Over-expression of EGFR has been linked with tumor malignancy such as invasion, angiogenesis, and metastasis (70-72). Elevated levels of EGFR are found on various types of solid tumors, such as breast, ovarian, lung, head and neck, prostate, and colorectal cancers, and have been proposed as prognostic markers for disease progression and drug resistance in chemotherapy (73-76). Therefore, EGFR has been recognized as a therapeutic target for cancer treatment.

The liposomal nanoparticles (liposomes and virosomes) are small vesicular carriers consisting of natural or synthetic lipids and additives enhancing delivery efficacy such as cationic polymers and viral fusogenic proteins. Liposomes encapsulate various therapeutic molecules including siRNAs. The liposomal carriers eventually break down through natural processes and spill their contents into certain tissues (19, 20). Lipoplexes was complexes of cationic liposomes and nucleic acids. They are good gene delivery systems for *in vitro* transfection (21), but not for *in vivo* transfection. Therefore, a great deal of efforts have been spent to improve *in vivo* gene trasfection efficiencies of liposomal systems. One of effors was development of virosomes containing fusogenic viral envelop proteins which were proven to be a more effective transfection system than conventional lipoplexes (25).

As far as anticancer siRNAs concerned, a number of cellular proteins essential in maintaining cell viability have been targeted. Among them,

vimentin and JAK3 have been extensively investigated as a target protein for dysregulation. Vimentin is a member of the type III intermediate filaments. Also, it is a marker of cells of mesenchymal origin such as fibroblasts and myofibroblasts. Vimentin intermediate filaments are soluble tetrameric polymers which are important structural proteins in motility, maintenance of cell shape, and endurance of stress in the cells (77, 78). It is also supporting structural integrity of quiescent cells as well as participating in adhesion, migration, survival, and varied cell signaling processes in activated cells (79). Vimentin-deficiency results in delayed wound healing in tissues (80). Therefore, the major challenges for vimentin siRNA application have been tested in *in vitro* and *in vivo* systems (81, 82).

Janus kinase (JAK) signaling pathways are instrumental for the differentiation, proliferation, and survival of cells (83). There are four members of the JAKs (JAK1, JAK2, JAK3, and Tyk2) constituting a subgroup of the intracellular nonreceptor tyrosine kinases in mammal cells. Recently, it has been demonstrated that JAK3 has a pivotal role in signal transduction by interacting with members of the STAT (signal transduction and activators of transcription) pathways, resulting in stimulation of cell proliferation (84. 85). The activating mutations in JAK3 have been identified as causes of cancers while inactivating mutations of JAK3 are known causes of immune deficiency (86). Hence, there have been many studies regarding JAK3-targeted gene therapy for cancer treatment (87).

At this moment, consequently, strategies targeting of vimentin and JAK3 siRNAs to EGFR overexpressing tumors by innovative immunonanoparticles can be a plausible option for anticancer gene therapy. The present study was designed to develop anti-EGFR immunonanoparticles (immunoliposomes, immunovirosomes, immunolipoplexes and immunoviroplexes) for targeted siRNA delivery to cancer cells overexpressing EGFR. Their siRNA delivery efficiencies were compared to each others in *in vitro* and *in vivo* systems. Antitumoral activities of vimentin and JAK3 siRNAs transferred by the anti-EGFR immunonanoparticles were also investigated in mice carrying tumors over-expressing EGFR. The systematic comparison of these delivery systems will provide useful information in terms of biophysical characteristics, target-directed binding and gene transfection *in vitro* and *in vivo*.

Ⅱ. MATERIALS AND METHODS

1. Materials

POPC, DSPE-PEG2000, DSPE-PEG2000-MAL, Rho-DOPE were purchased from Avanti Polar Lipid, Inc. (Alabaster, USA). PD-10 column and Sepharose CL-4B were purchased from Amersham Bioscience (Uppsala, Sweden). Amicon Ultra-4 30K and 50K MWCO were purchased from Amicon (Beverly, Sweden). DMKE cationic lipid was chemically synthesized by Dr. Jang (Department of Chemistry and Medicinal Chemistry, Yonsei University, Korea).

2. Cells and cell culture

Human adenocarcinomic alveolar basal epithelial A549, human ovarian cacinoma SK-OV-3, human breast adenocalcinoma MCF-7 cells and mouse melanoma B16BL6 cells were purchased from the American Type Culture Collection. SK-OV-3 cells were maintained as monolayer cultures in DMEM/F12 (Gibco), A549 cells in RPMI 1640, MCF-7 cells in DMEM, and B16BL6 cells in MEM. SK-OV-3 and A549 cells were EGFR-positive cell lines while MCF-7 and B16BL6 cells were not. The culture media were supplemented with 10% heat-inactivated fetal bovine serum (Gibco) and 100 units/㎖ penicillin and 100 ㎍/㎖ streptomycin (Gibco). The cells were cultured in a humidified atmosphere of 95% air and 5% CO_2 at 37℃.

3. siRNA preparation

The FITC-labeled control siRNA was synthesized and purified by Bioneer co. (SN-1023). The FITC-labeled siRNA was 21-mer of sense/antisense duplex with the following sequence; 5'-CCUACGCCACCAAUUUCGU-3' (sense) and 5'-ACGAAAUUGG UGGCGUAGG-3' (antisense). Luciferase siRNA (GP-RNA1041) and vimentin siRNA (GP-RNA1015) were provided by Genolution Pharmaceuticals Inc. (Seoul, Korea). JAK3 siRNA (VHS41248) were provided by Invitrogen.

4. Purification of Sendai virus F/HN protein

As described in the previous chapter, Sendia virus F/HN proteins were purified from the cultured Sendai virus and then formulated into liposomes to prepare virosomes. Briefly, the Sendai virus cultured in the allantoic fluid of egg embryo was pelleted. The virus was resuspended in 2 ml of PBS containing 1% Triton X-100, followed by incubation at 20℃ for 2 h and centrifugation at 100,000 g for 1 h at 4℃ to remove the detergent-insoluble substances. The detergent was removed by stepwise addition of SM2 Bio-Beads (Bio-Rad Lab.) and the final turbid suspension containing F/HN proteins was then separated.

5. Preparation of immunonanoparticles

5-1. Preparation of liposomes and virosomes encapsulating siRNA

DMKE (5 mole%), POPC (91 mole%), DSPE-PEG_{2000} (3.8 mole%), DSPE-PEG_{2000}-MAL (0.2 mole%) and Rho-DOPE (0.1 mole%) were dissolved in chloroform and methanol mixture (2:1, v/v). The organic solvent was evaporated under a stream of N_2 gas. Vacuum desiccation for 2 h ensured removal of the residual organic solvent and dry. The dried films of 2 mg lipids were hydrated in 1 ml of 0.1 M phosphate buffer (pH 5.5) containing siRNA (10:1, lipid wt:siRNA wt) and then vigorously mixed by a vortex mixer for 5 min. After hydration, the liposomes were repeated 10 cycles of freezing and thawing, and extruded 10 times through a polycarbonate membrane with a pore size from 800 nm to 80 nm using a extruder (Avanti Polar Lipids,). The virosomes were prepared as described previously.

5-2. Preparation of cationic liposomes and cationic virosomes

DMKE (48 mole%), cholesterol (48 mole%), DSPE-PEG_{2000} (3.8 mole%), DSPE-PEG_{2000}-MAL (0.2 mole%) and Rho-DOPE (0.1 mole%) were dissolved in the chloroform and methanol mixture (2:1, v/v). The organic solvent was evaporated under a stream of N_2 gas, followed by vacuum desiccation of 2 h. The dried lipid films (2 mg lipid) were hydrated in 1 ml of 0.1 M phosphate buffer (pH 7.2) and then vigorously mixed by vortexing. After hydration, the resulting suspension was subjected to 10 cycles of freezing and thawing, and extruded 10 times through a polycarbonate membrane with a pore size of 80 nm using a extruder. Protamine sulfate (PS)-condensed siRNA-encapsulating cationic lipoplexes and viroplexes were prepared by precomplexation of siRNA with PS (0.35:1 siRNA wt:PS wt) for 30 min at room temperature.

Lipoplexes of siRNA and cationic liposomes were prepared by gentle mixing of PS-condensed siRNA and the cationic liposomes (DMKE/Chol) solution at various N/P ratios of siRNA/lipid. After incubation of the lipoplexes for 30 min at room temperature, Sendai viral F/HN proteins (1:1 DNA wt:F/HN protein wt) were added and additionally incubated for 15 min at room temperature with gentle mixing. The resulting complex is called viroplexes.

5-3. Conjugation of anti-EGFR antibody to nanoparticles

Cetuximab were thiolated for 1 h at room temperature by reacting with Traut's reagent in degassed phosphate buffer (0.1 M, 2 mM EDTA, pH 8.0). Unreacted Traut's reagents were removed by passing through PD-10 column with the degassed phosphate buffer. The thiolated antibodies were conjugated to the maleimide groups at the distal-termini of PEG chains on the nanoparticles. Briefly, thiolated antibody solution was added to the liposome or lipoplex solutions (0.2:1, a mole ratio of Ab ad maleimide), and then incubated for 20 h at 4℃ with continuous shaking. Unconjugated antibodies were separated from the nanoparticles by chromatography through a Sepharose CL-4B column in phosphate buffer (0.1 M, pH 7.2).

Table Ⅰ. Components of anti-EGFR immunonanoparticles

<table>
<tr><th>Components</th><th colspan="2">Rationale</th></tr>
<tr><td>Antibody;
Cetuximab (Erbitux®)</td><td colspan="2">It was used for targeting to EGFR in various cells and to enhance selective intracellular delivery.</td></tr>
<tr><td>Linkage;
DSPE-PEG₂₀₀₀-MAL
+ Antibody</td><td colspan="2">The sulfhydryl groups (SH-) in whole antibody were conjugated to liposomes and lipoplexes via a maleimide moiety for targeted binding and internalization</td></tr>
<tr><td>DMKE</td><td colspan="2">It was used for effective pDNA encapsulation or complexation with liposomes via charge interaction.</td></tr>
<tr><td rowspan="4">Nanoparticles</td><td>Liposomes and virosomes</td><td>Lipoplexes and viroplexes</td></tr>
<tr><td>Neutrally charged for in vivo stability</td><td>Positively charged for effective cell binding</td></tr>
<tr><td colspan="2">PEGylated for longer circulation</td></tr>
<tr><td colspan="2">Small diameter for efficient extravasation</td></tr>
<tr><td>Sendai viral F/HN proteins</td><td colspan="2">They were inserted to increase membrane fusogenecity in virosomes and viroplexes</td></tr>
<tr><td>Agent;
Nucleic acids</td><td colspan="2">FITC-labeled control siRNA,
vimentin siRNA and JAK3 siRNA</td></tr>
</table>

6. Gel retardation analysis of anti-EGFR immunonano particles with siRNA

To ensure complete siRNA complexation with anti-EGFR immunonano particles and insertion of Sendai viral F/HN proteins to make immunovirosomes and immunoviroplexes, the gel retardation analysis was performed using agarose gel electrophoresis. As mentioned earlier, the immunonanoparticles (immunoliposomes, immunovirosomes, immunolipoplexes and immunoviroplexes) prepared under varied conditions (1 ㎍ siRNA, 70 pmole) were run on 1% agarose gel and siRNA bands were visualized by UV illumination. An appropriate N/P ratio of siRNA complexation and the amount of encapsulated siRNA were quantified by the Quantity one program of Gel Doc EQ system.

7. Analysis of vesicle size and surface charge of anti-EGFR immunonanoparticles containing siRNA

To observe the changes of vesicular size and surface charge of the nanoparticles during siRNA encapsulation (or complexation) and antibody-coupling, the vesicular size and ζ-potential were measured using a particle analyzer. All the samples (100 ㎍ lipid/㎖) were placed into the specimen holder of a Zetamaster S 5 min prior to measurement in order to allow equilibration to room temperature.

8. Flow cytometry analysis of anti-EGFR immunonano particles containing siRNA

Specific cellular binding affinities and siRNA delivery efficiencies of rhodamine-labeled anti-EGFR immunonanoparticles containing FITC-labeled control siRNA were evaluated in SK-OV-3, A549, MCF-7 and B16BL6 cells (each 4×10^5/well) in 6-well plates. The tumor cells treated with the double-labeled anti-EGFR immunonanoparticles for 30 min at room temperature were typsinized. After washed with PBS, the cells then treated with 0.2% paraformaldehyde for 5 min at room temperature in dark. Then, the cells were counted by flow cytometry analysis.

In order to show the EGFR-mediated siRNA transfection, The cells were pretreated with free Cetuximab (1 ㎍/ml each well) for 30 min, The pretreated cells were transfected with the immunonanoparticles containing FITC-labeled siRNA (1 ㎍; 70 pmole/ml) for 30 min at room temperature. The cells were typsinized and then treated with 0.2% paraformaldehyde for 5 min at room temperature in dark. The fixed cells were counted by flow cytometry analysis.

9. *In vitro* siRNA transfection by anti-EGFR immunonano particles

In vitro transfection with the anti-EGFR immunonanoparticles containing siRNA were performed in SK-OV-3, A549, MCF-7 or B16BL6 cells in 24-well plates. The prepared anti-EGFR immunonanoparticles containing siRNA prepared under optimal conditions (12:1, 9:1, 1:6 and 1:3; respective N/P ratios of andimmunoliposomes, immunovirosomes, immunolipoplexes and immunoviroplexes) were added to the tumor cells (each 4×10^4/well, final concentration of luciferase siRNA; 20 nM). After transfection for 4 h and the transfected cells were additionally incubated in fresh 10% FBS-containing media for 24 h at 37℃. The transfected cells were washed twice with PBS (pH 7.4) and lysed with 200 ㎕ of lysis buffer (1% Triton X-100, 1 mM dithiothreitol and 2 mM EDTA, pH 7.8) for 2 h at room temperature with gentle agitation. The plates were incubated at -20℃ for 20 min and thawed at room temperature. The cell lysates were centrifuged for 20 min at 4℃ and 12,000 rpm to pellet debris. Luciferase activities in the supernatant were measured with a luciferase assay kit and a luminometer, Minilumat LB9506 (Berthold Technologies, Bad Wildbad, Germany). The protein concentration of the supernatant was measured with the DC Protein Assay Kit. The data were expressed as RLU of luciferase/㎎ of total cellular proteins.

10. cytotoxicity assay of anti-EGFR immunonanoparticles containing anti-cancer siRNA

Cytotoxcicity of anti-EGFR immunonanoparticles containing siRNA was determined by propidium iodide (PI) staining. SK-OV-3 and A549 cells were plated into 6-well plates (each 4×10^5/well) and cultured for 24 h. The tumor cells were treated with various concentrations of siRNA-containing (10 nM and 20 nM) anti-EGFR immunonanoparticles and then cultured for 24 h. After typsinization, 2 ㎕ of PI solution (50 ㎍/㎖) was added to the cells followed by flow cytometry analysis.

11. Reverse-transcriptase PCR analysis of mRNA levels of vimentin

The prepared anti-EGFR immunonanoparticles containing vimentin siRNA were added to SK-OV-3, A549, MCF-7 and B16BL6 cells (each 4×10^5/well, 20 nM of vimentin siRNA). After transfection as described above, the transfected cells were washed twice with PBS (pH 7.4) and treated with Trizol (Invitrogen, Eugene, USA) to extract all RNA. Reverse-transcriptase PCR (polymerase chain reaction) was preformd using 2 ㎍ of the extracted RNA and random primers, the MMLV reverse transcriptase (Invitrogen, Eugene, USA) and the G-*Taq* kit (Cosmo GENTECH, Seoul, Korea). Forward and reverse primers (Cosmo GENTECH, Seoul, Korea) were as follows, the forward primer of vimentin ; 5'-TGGATTCACTCCCTCTGGTT-3', the reverse primer of vimentin; 5'-GGTCATCGTGATGCTGAGAA-3', and the forward primer of control GAPDH; 5'-CGGGAAGCTTGTGATCAATGG-3', the reverse primer of control GAPDH; 5'-GGCAGTGATGGCATGGACTG-3'). Reverse transcription was performed at 70 ℃ for 15 min. The reverse transcripts were run on 2% agarose gel.

12. Localization of anti-EGFR immunonanoparticles containing siRNA in tumor tissues

The anti-EGFR immunonanoparticles containing rhodamine-DOPE (0.1 mole%) were intravenously injected to BALB/c nude mice carrying SK-OV-3 tumors. Tumor tissues were excised 1 day post administration. The removed tumors were immediately frozen, transversally sectioned (3 ㎛) then examined by fluorescence microscopy (×100).

13. *In vivo* tumor growth inhibition by administration of the anti-EGFR immunonanoparticles containing vimentin and/or JAK3 siRNAs

Female BALB/c nude mice (4~5 week-old) were subcutaneously injected with 1×10^7 of SK-OV-3 cells on the abdomen right quadrant. When the tumors grew to approximately 50 ㎣ of volume (length×width^2/2), the mice were intravenously or intratumorally injected with the anti-EGFR immunonanopaticles (injection volumes: 200 ㎕ for the intravenous, 100 ㎕ for the intratumoral) (n=5) containing vimentin and/or JAK3 siRNAs (0.5 mg siRNA/kg, 10 ㎍ of siRNA per mouse). In a separated set of animal experiment, doxorubicin (15 mg/kg) was intravenously co-injected to the mice, treated with the anti-EGFR immunonanopaticles containing vimentin and/or JAK3 siRNAs, at the same injection days. Tumor growth was monitored for 37 days post treatment. The mice were sacrificed on day 43 and the lung colonization was counted.

Ⅲ. RESULTS

1. Preparation of four-different anti-EGFR immunonano particles containing siRNA

As shown in Figure 1, anti-EGFR antibody Cetuximab was conjugated to the surfaces of four different liposomal delivery systems (immunoliposomes, immunovirosomes, immunolipoplexes and immunoviroplexes) by the direct coupling method. Thiolated Cetuximab antibodies were conjugated to reactive PEG termini exposed on neutral liposomes or cationic liposomes. The analysis of gel filtration chromatography showed effective conjugation of the antibody molecules to the liposomal surface. The Ab conjugation reaction was almost completed at 0.2:1 molar ratio of Ab and DSPE-PEG_{2000}-Mal (Figure 2).

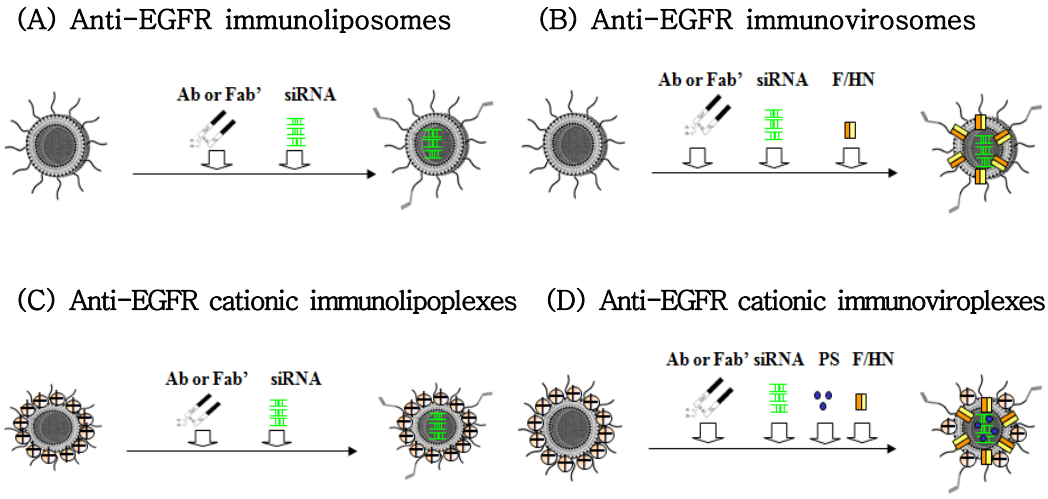

Figure 1. Schematic illustration of anti-EGFR immunonano particles with siRNA.

(A) Immunoliposomes were prepared by coupling of thiolated antibodies neutrally charged immunoliposomes followed by siRNA encapsulation. (B) Immunoliposomes were preparec by insertion of Sendai viral F/HN protein into neutrally charged immunoliposomes. (C) Immunolipoplexes were prepared by coupling of thiolated antibodies to cationic liposomes followed by siRNA complexation. (D) Immunoviroplexes were prepared by insertion of Sendai viral F/HN proteins into cationic lipoplexes.

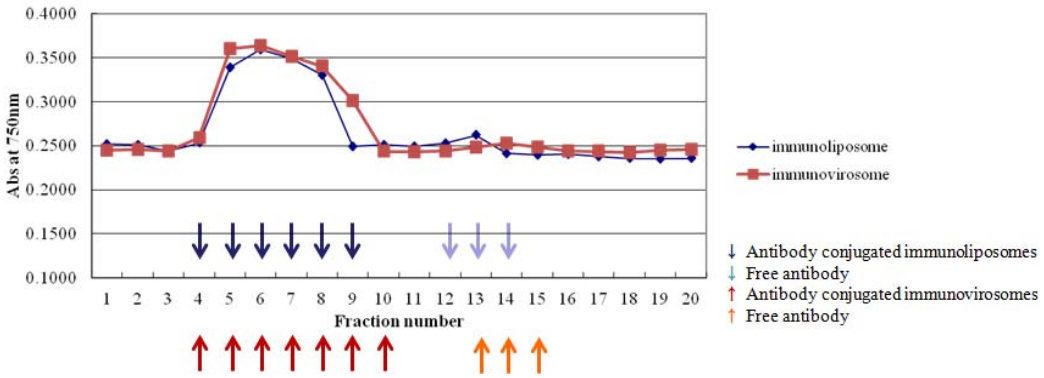

Figure 2. Elution profiles of anti-EGFR immunonanoparticles and unbound antibodies.

The reaction mixtures of nanoparticles (liposomes and virosomes) and Cetuximab antibodies were loaded onto a Sepharose CL-4B gel filtration column and eluted with 0.1 M phosphate buffer (pH 7.2). The antibody concentration of each fraction (1 ml) were quantified by protein assay.

2. Preparation of anti-EGFR immunoliposomes and immuno virosomes encapsulating siRNA

The prepared immunoliposomes were mixed with a buffer containing siRNA at various ratios of liposome and siRNA. To verify siRNA encapsulation into liposomes, the liposomes and virosomes prepared at 1:1~12:1 N/P ratios of cationic liposomes and siRNA were run on 1% agarose gel (Figure 3). According to the gel retardation test, complete encapsulation of siRNA into liposomes was seen at 9:1 or higher N/P ratios (Figure 3A). Complete encapsultation of siRNA into virosomes was seen at 6:1 and higher ratios (Figure 3B). Therefore, all liposomes and virosomes utilized in this study were formulated at 12:1 and 9:1 N/P ratios, respectively, otherwise mentioned.

(A) Anti-EGFR immunoliposomes

(B) Anti-EGFR immunovirosomes

(N/P ratio)

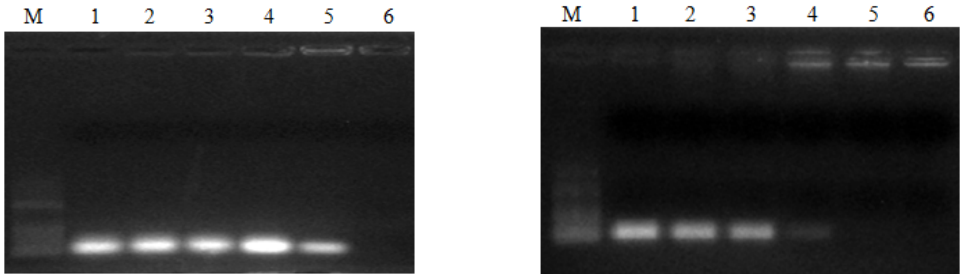

Figure 3. Encapsulation of siRNA into anti-EGFR immuno liposomes and immunovirosomes.

The prepared anti-EGFR liposomes (A) and anti-EGFR virosomes (B) encapsulating siRNA were run on 1% agarose gel and visualized by UV illumination. Lane M; 100 bp molecular weight markers, lane 1; free siRNA, lane 2; 1:1 N/P ratio, lane 3; 3:1 N/P ratio, lane 4; 6:1 N/P ratio, lane 5; 9:1 N/P ratio, lane 6; 12:1 N/P ratio.

3. Preparation of anti-EGFR immunolipoplexes and immuno viroplexes

The cationic liposomes were mixed with a buffer containing siRNA at varied ratios of cationic liposome and siRNA. To verify complete siRNA complexation with cationic liposomes or virosomes, the lipoplexes or viroplexes prepared at 1:1~12:1 N/P ratios of cationic liposome and siRNA were run on 1% agarose gel (Figure 4). According to the gel retardation test, complete complexation of DMKE/Chol cationic liposomes and siRNA and was seen at 3:1 and a lower N/P ratios (Figure 4A). Complete complexation of cationic virosomes and siRNA was seen at 1:1 and lower ratios (Figure 4B). Therefore, all lipoplexes and viroplexes utilized in this study were formulated at 6:1 and 3:1 N/P ratios, respectively, otherwise mentioned.

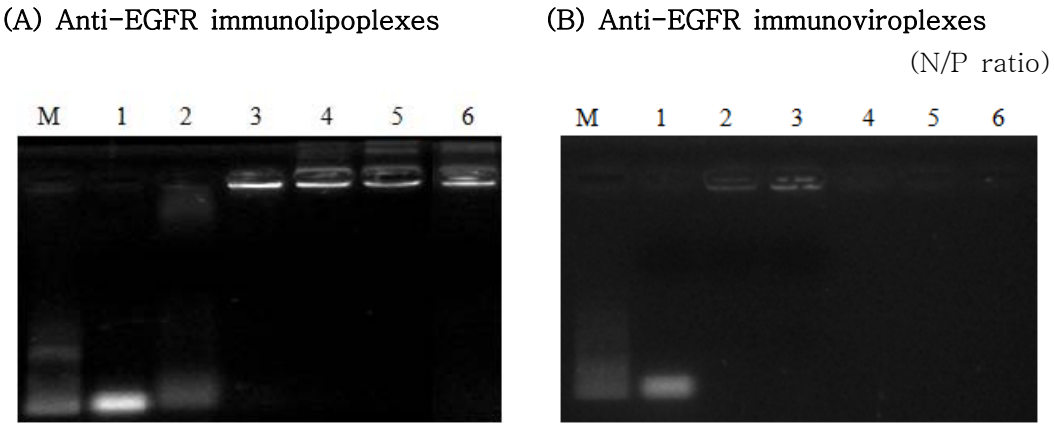

Figure 4. Complexation of siRNA with anti-EGFR cationic immunolipoplexes and immunoviroplexes.

The cationic liposomes (A) and virosomes (B) complxed with siRNA under varied conditions were run on 1% agarose gel and visualized by UV illumination. Lane M; 100 bp molecular weight markers, lane 1; free siRNA, lane 2; 1:1 N/P ratio, lane 3; 3:1 N/P ratio, lane 4; 6:1 N/P ratio, lane 5; 9:1 N/P ratio, lane 6; 12:1 N/P ratio.

4. Vesicular size and surface charge of anti-EGFR immuno nanoparticles containing siRNA

As shown in Table III of the previous chapter, vesicular sizes of liposomes and virosomes were slightly increased by siRNA encapsulation (or complexation), regardless of surface charge. Also, pDNA encapsulation slightly reduced the surface charge of the liposomes and virosomes. Meanwhile, pDNA addition slightly reduced the sizes of immunonanoparticles except the cationic immunovirosomes. The same procedure slightly reduced the surface charges of all the immunonanoparticles in general.

Addition of F/HN proteins to liposomal vesicles increased the sizes of liposomes and lipoplexes as same as the previous results. The sizes of immunonanoparticles were bigger than the nanoparticles without antibodies. All of the finalized anti-EGFR immunonanoparticles exhibited appropriate vesicular sizes smaller than 220 nm for *in vivo* transfection.

Table Ⅱ. Vesicular size and surface charge of anti-EGFR immunonanoparticles containing siRNA

Anti-EGFR immunonanoparteicles			Size (㎚)*	Zeta- potential (㎷)*
No mAb	No siRNA	Neutral liposomes	130.8 (± 3.0)**	8.2 (± 1.0)**
		cationic liposomes	98.6 (± 3.0)	56.7 (± 6.0)
		Neutral virosomes	156.3 (± 4.5)	5.8 (± 0.5)
		cationic virosomes	121.8 (± 2.3)	45.2 (± 2.7)
	with siRNA	Neutral liposomes	151.8 (± 8.9)	-3.3 (± 0.2)
		cationic lipoplexes	135.6 (± 1.0)	50.9 (± 0.3)
		Neutral virosomes	192.1 (± 2.1)	-1.9 (± 0.5)
		cationic viroplexes	136.8 (± 9.2)	38.5 (± 1.0)
with mAb	no siRNA	Anti-EGFR neutral immunoliposomes	182.8 (± 10.6)	2.1 (± 0.5)
		Anti-EGFR cationic immunoliposomes	131.3 (± 2.9)	45.4 (± 0.4)
		Anti-EGFR neutral immunovirosomes	230.7 (± 7.6)	0.5 (± 0.9)
		Anti-EGFR cationic immunovirosomes	184.6 (± 2.7)	42.1 (± 1.0)
	with siRNA	Anti-EGFR neutral immunoliposomes	173.1 (± 7.5)	-4.9 (± 0.5)
		Anti-EGFR cationic immunolipoplexes	153.1 (± 4.2)	25.4 (± 1.2)
		Anti-EGFR neutral immunovirosomes	213.5 (± 8.1)	-2.3 (± 0.4)
		Anti-EGFR cationic immunoviroplexes	179.4 (± 3.7)	21.6 (± 0.7)

* The particle size and zeta-potentials were measured 4 times using a zetasizer.

** The particles size (㎚); average particle size ± S.D.
zeta-potentials (㎷); average zeta-potentials ± S.D.

5. *In vitro* cellular binding of anti-EGFR immunonano particles containing siRNA

Specific cellular binding of anti-EGFR immunonanoparticles containing FITC-labeled siRNA to four different types of cancer cells (SK-OV-3, A549, MCF-7 and B16BL6) were analysed by flow cytometry (Figure 5A). As speculated, regardless of types of nanoparticles, all of the anti-EGFR immunonanoparticles showed high cellular binding to EGFR-positive cell lines (A549 and SK-OV-3 cells). Meanwhile, the same anti-EGFR immunonanoparticles had lower binding affinity to EGFR-negative cell lines (MCF-7 and B16BL6 cells).

To verify their EGFR-mediated binding to tumor cells, the tumor cells were pretreated with anti-EGFR antibody (Cetuximab) before transfection. Then, the pretreated cells were incubated in the presence of the anti-EGFR immunonanoparticles. Binding of the anti-EGFR immunonanoparticles to the EGFR-positive cells (SK-OV-3 and A549) were significantly inhibited by treatment with free Cetuximab (Figure 5B). Meanwhile, there was no significant reduction of binding of the anti-EGFR immunonanoparticles to EGFR-negative cells (MCF-7 and B16BL6) by free Cetuximab treatment.

(A)

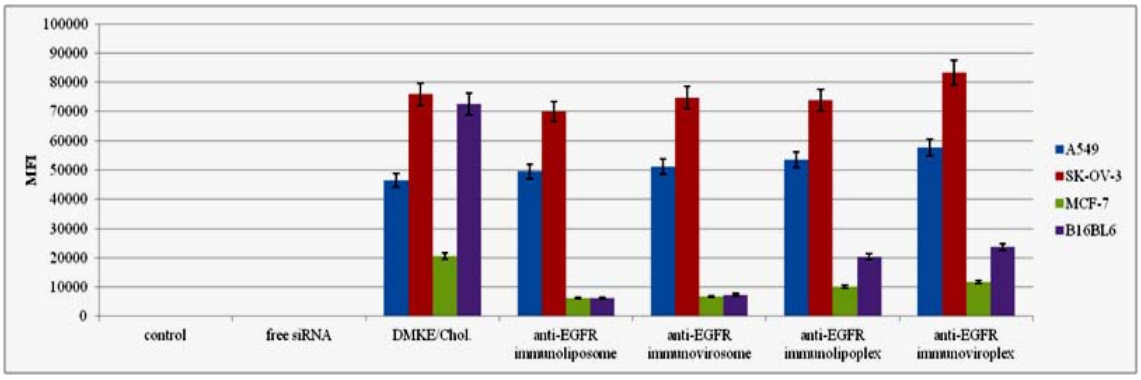

(B)

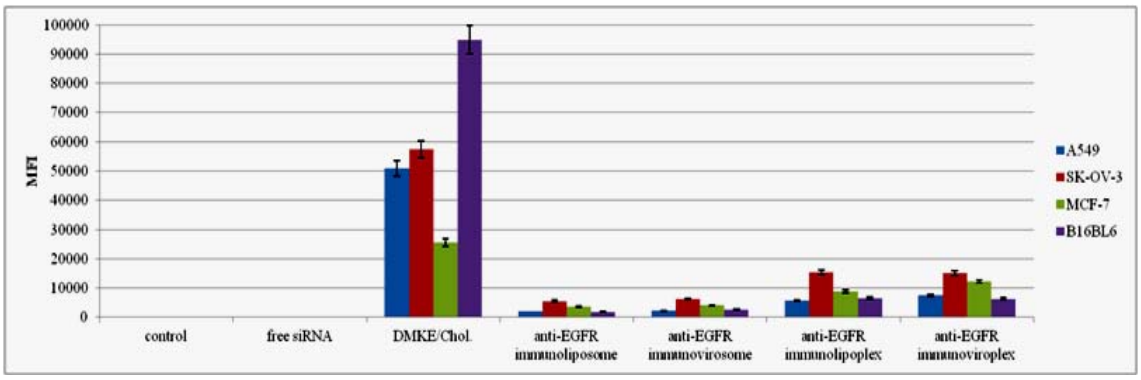

Figure 5. *In vitro* binding of the anti-EGFR immunonano particles containing siRNA to tumor cells.

(A) The cancer cells (SK-OV-3, A549, MCF-7 and B16BL6) were incubated with the anti-EGFR immunonanoparticles containing FITC-labeled siRNA for 30 min at 4℃. (B) The same cells were pretreated with free Cetuximab antibodies followed by incubation with the anti-EGFR immunonanoparticles containing FITC-labeled siRNA. After washed with PBS, the cells were analysed by flow cytometry (n=3). MFI; mean fluorescence of intensity, control; untreated.

6. *In vitro* siRNA transfection by anti-EGFR immunonano particles

Luciferase siRNA was transferred to A549, SK-OV-3, MCF-7 and B16BL6 cells via the anti-EGFR immunonanoparticles. There was significant reduction of luciferase expression by luciferase siRNA transfection in the EGFR-positive A549 and SK-OV-3 cells, but much less reduction in EGFR-negative MCF-7 and B16BL6 cells (Figure 6). The reduction levels of luciferase expression appeared to be dependent upon the expression levels of EGFR on the tumor cell surface. The anti-EGFR immunolipoplexes and immuno viroplexes were more effective in reduction of target gene expression. In contrast, the conventional catonic lipoplexes (Lipofectamine 2000 and DMKE/Chol) showed effective siRNA transfection to all types of tumor cells.

To verify EGFR-mediated transfection of the immunonanoparticles, the cells were pretreated with free Cetuximab antibodies followed by transfection with the anti-EGFR immunonanoparticles containing luciferase siRNA. The pretreatment with Cetuximab was able to inhibit luciferase siRNA tansfecton to SK-OV-3 and A549 cells, resulting in less reduction of luciferase expression (Figure 6). Meanwhile, the same treatment hardly affect the levels of luciferase expression in MCF-7 and B16BL6 cells.

(A) A549

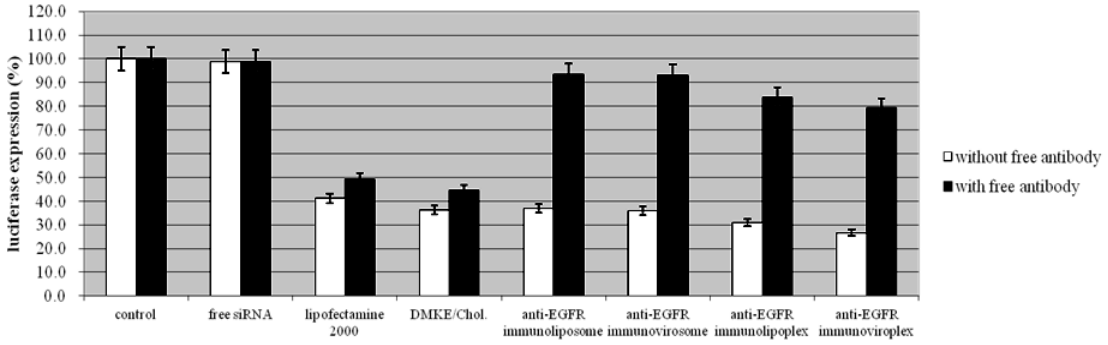

(B) SK-OV-3

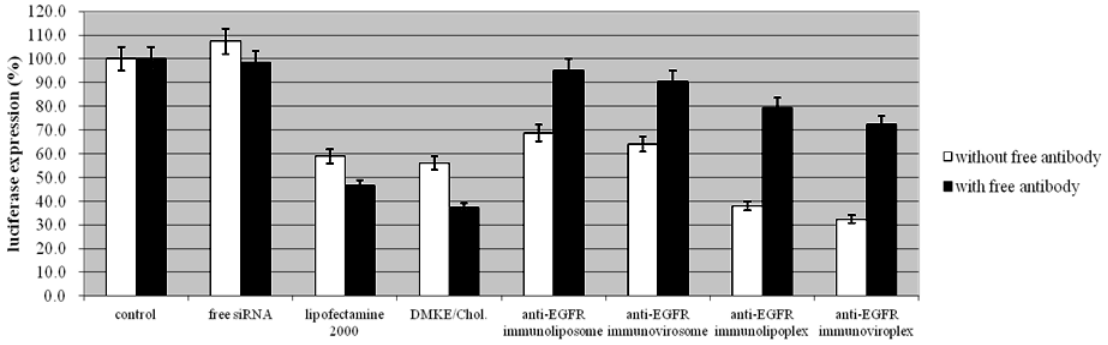

(C) MCF-7

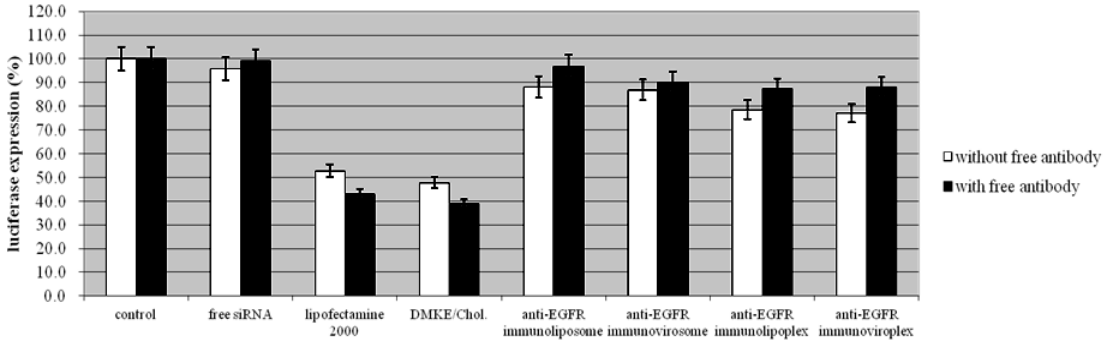

(D) B16BL6

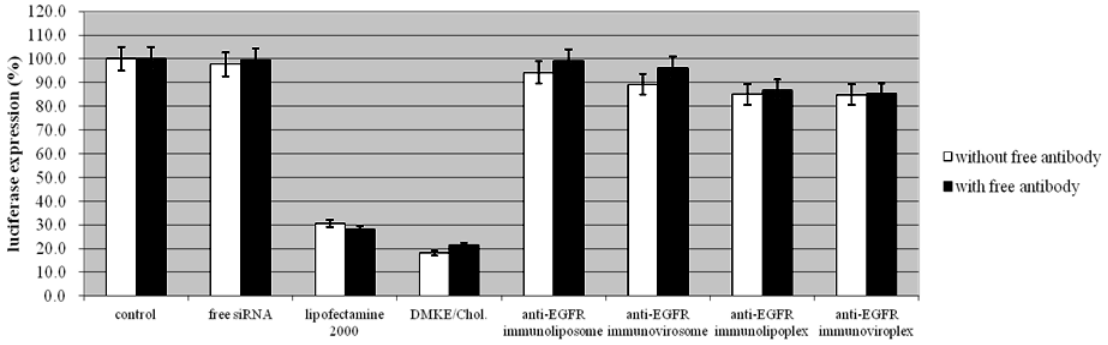

Figure 6. *In vitro* luciferase siRNA transfection by anti-EGFR immunonanoparticles.

The anti-EGFR immunonanoparticles (immunoliposomes, immunovirosomes, immunolipoplexes, and immunoviroplexes) containing luciferase siRNA were transfected to A549 (A), SK-OV-3 (B), MCF-7 (C) and B16BL6 (D) cells pretransfected with pAAVCMV-Luc in 24-well plates (each 4×10^5/well). Also the same cells were pretreated with free Cetuximab antibodies for 30 min and then transfected with the anti-EGFR immunonanoparticles containing luciferase siRNA. After 4 h transfection, the cells were further incubated for 24 h. Luciferase expression in the cells was calculated to RLU per milligram of proteins. Each bar represents the mean ± S.D. for three separate experiments of luciferase assay.

7. *In vitro* cytotoxicity of anti-cancer siRNA

The DMKE/Chol cationic lipoplexes containing a various anti-cancer siRNA were incubated in A549 (A) and SK-OV-3 (B) cells to measure their cell toxicity by trypan blue staining. Among the anti-cancer siRNA, vimentin siRNA and JAK3 siRNA combination showed severe damage to the cultured cell lines, exhibiting 35% ~ 50% cell cytotoxicity (Figure 7).

(A) A549

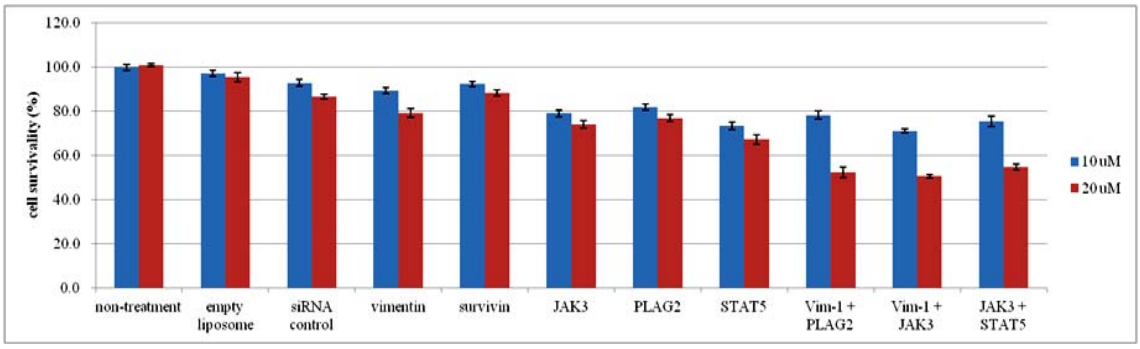

(B) SK-OV-3

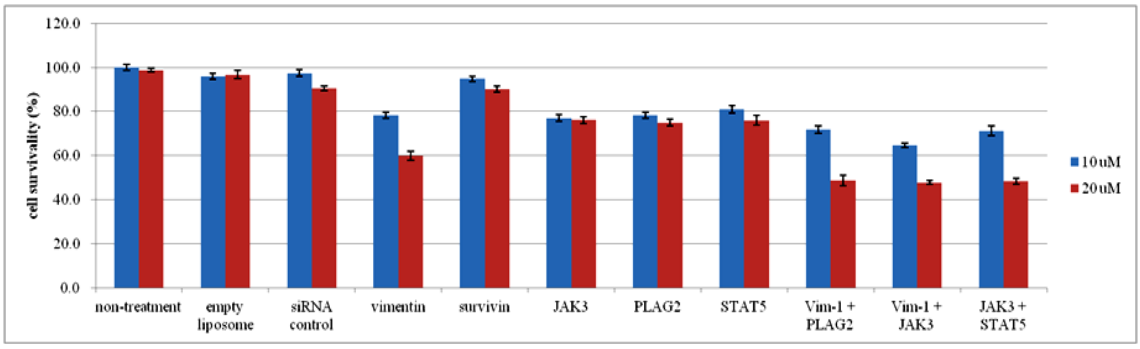

Figure 7. *In vitro* cytotoxicity of anti-cancer siRNA.

A549 (A) and SK-OV-3 (B) cells were treated with varied combinations of siRNAs using DMKE/Chol cationic liposomes. Cell viability was measured by the PI staining assay 24 h later.

8. *In vitro* vimentin siRNA transfection mediated by anti-EGFR immunonanoparticles

Vimentin siRNA was formulated in the anti-EGFR immunolipoplexes and immunoviroplexes, which showed the most effective siRNA transfection to tumor cells expressing EGFR. A549, SK-OV-3, MCF-7, and B16BL6 cells were transfected using the prepared anti-EGFR immunonanoparticles or control carriers containing vimentin siRNA. After 4 h transfection and 12 h additional incubation, the levels of vimentin mRNA were determined by RT-PCR and Quantity one program. According to the experimental results (Figure 8), the levels of vimentin mRNA in A549 and SK-OV-3 cells were reduced by vimentin siRNA transfection mediated by the immunolipoplexes and immunoviroplexes. However, the same systems little affected the vimentin mRNA level in B16BL6 cells. These data imply that the anti-EGFR immunolipoplexes and immunoviroplexes were able to effectively deliver vimentin siRNA to tumor cells overexpressing EGFR. Among the two systems, the anti-EGFR immunoviroplexes appeared to be more effective in siRNA transfection, exhibiting approximately 20~65% higher transfection under the same transfection conditions. The MCF-7 cells is known to be vimentin-negative.

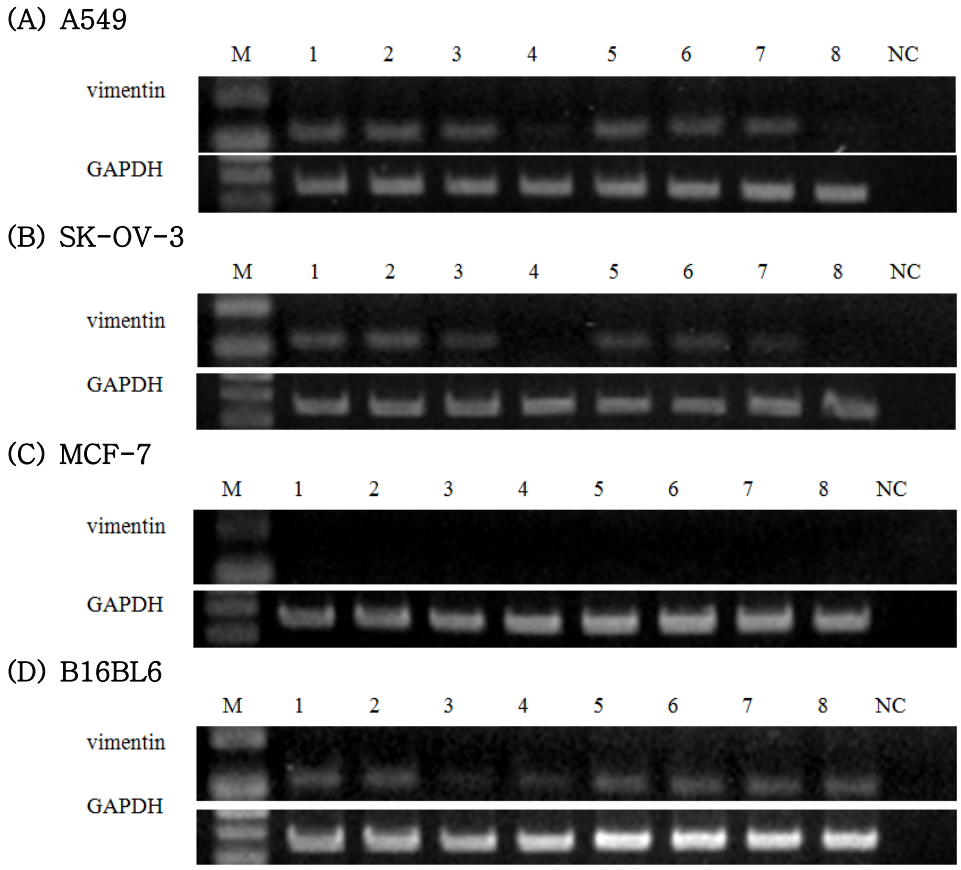

Figure 8. *In vitro* vimentin siRNA transfection by anti-EGFR immunonanoparticles.

A549, SK-OV-3, MCF-7 and B16BL6 cells were transfection with free vimentin siRNA (lane 1, 5) or vimentin siRNA in cationic lipoplexes (lane 2), PEG-lipoplexes (lane 3), anti-EGFR immunolipoplexes (lane 4), cationic viroplexes (lane 6), PEG-viroplexes (lane 7), and anti-EGFR immunoviroplexes (lane 8). After 4 h transfection and 12 h additional incubation, vimentin mRNA levels in the transfected cells was measured by RT-PCR.

9. Tumor localization of anti-EGFR immunonanoparticles containing siRNA intravenously administered

The rhodamine-labeled anti-EGFR immunonanoparticles (immunoliposomes, immunovirosomes, immunolipoplexes and immunoviroplexes) were intravenously injected to BALB/c nude mice carrying SK-OV-3 tumors. Then, cryosections of the xenografted SK-OV-3 tumors were examined by fluorescence microscopy. Commonly, all types of the anti-EGFR immunonanoparticles showed effective localization in the tumor tissues compared with the control DMKE/Chol lipoplexes (Figure 9). Among the anti-EGFR immunonanoparticles, the anti-EGFR immunolipoplexes and immunoviroplexes showed more effective localization than the others.

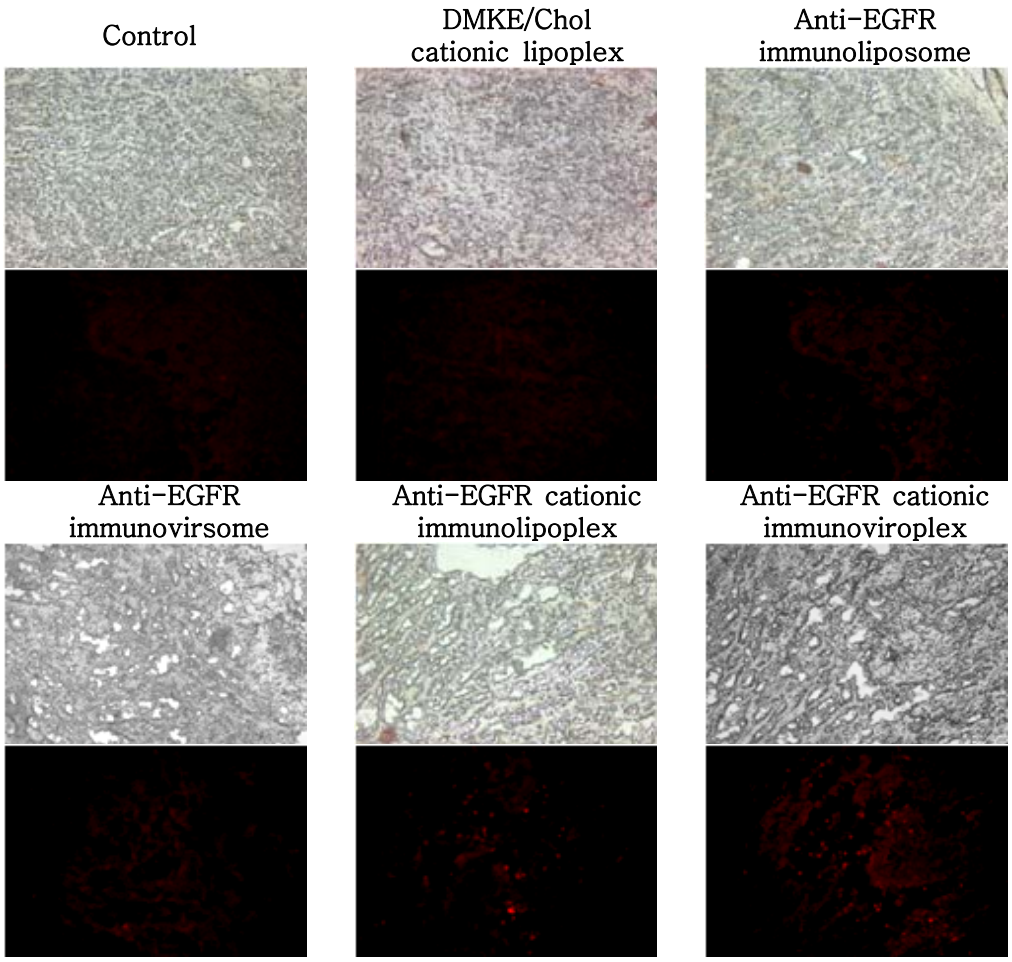

Figure 9. *In vivo* Localization of anti-EGFR immunonano particles containing siRNA in tumor tissues.

Rhodamine-labeled cationic lipoplexes and anti-EGFR immunonanoparticles containing siRNA were intravenously administered to mice carrying SK-OV-3 (tumor volume ~100 ㎣). The localization of the immunonanoparticles in tumor tissues was observed under a fluorescence microscope 24 h post injection (×100).

10. SK-OV-3 tumor growth inhibition by administration of anti-EGFR immunonanoparticles containing vimentin and/or JAK3 siRNAs

The anti-EGFR anti-EGFR immunolipoplexes and immunoviroplexes, which were proven to be effective in *in vivo* siRNA transfection to tumors overexpressing EGFR, were carefully formulated with vimentin and/or JAK3 siRNAs. Mice carrying SK-OV-3 tumors were treated with the prepared anti-EGFR immunonanoparticles four times at intervals of 3 days. In the first set of animal experiment, the anti-EGFR immunonanoparticles containing vimentin and/or JAK3 siRNAs were intravenously administered to mice carrying via tail vain (Figure 10). In the second experiment, the mice carrying tumors were treated by combinations of the same immunonanoparticles and doxorubicin (Figure 11). For 37 days of observation, significant inhibition of the tumor growth was seen in all the treated mice with the tendency of tumor growth inhibition becoming apparent with days (Figure 10). Cotransfection of vimentin and JAK3 siRNAs more effectively inhibited tumor growth and metastasis than administration of either gene alone.

The intratumorally administered anti-EGFR immunolipoplexes (or immunoviroplexes) containing vimentin and JAK3 siRNAs were also effective in inhibition in tumor growth and metastasis than the carriers without the antibody (Figure 11). Compared with the untreated one, the mice treated with the anti-EGFR immunolipoplexes or immunoviroplexes with the two siRNAs exhibited an approximately 42% and 75% reduction of tumor growth on day 37 post tumor inoculation, respectively. In addition, intravenous administration of doxorubicin synergistically enhanced the antitumoral efficacy of the anti-EGFR immunolipoplexes and immunoviroplexes containing vimentin and JAK3 siRNA. Compared with administration of only the anti-EGFR immunonanoparticles containing the two siRNAs, the additional doxorubicin treatment further inhibited tumor growth by 99.8%. Three mice out of 5 tumor-carrying mice showed complete tumor regression and no pulmonary metastasis by treatment with doxorubicin and the immunoviroplexes.

(A) Tumor volume

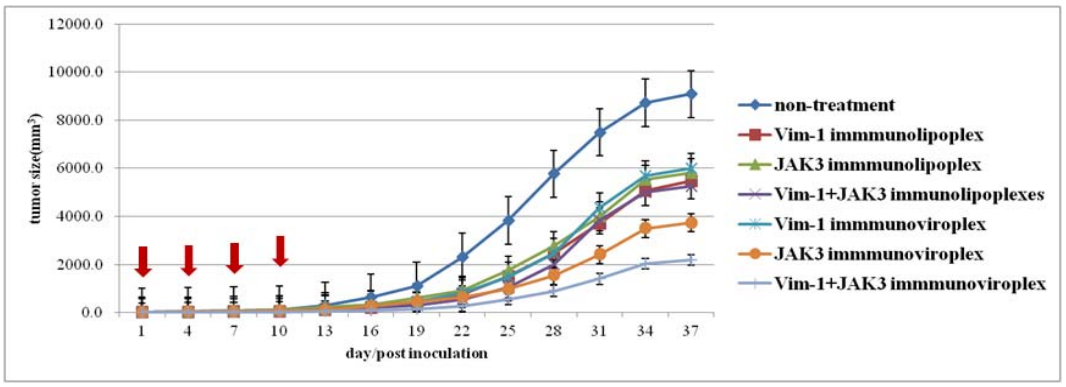

(B) Counting of lung tumor colony

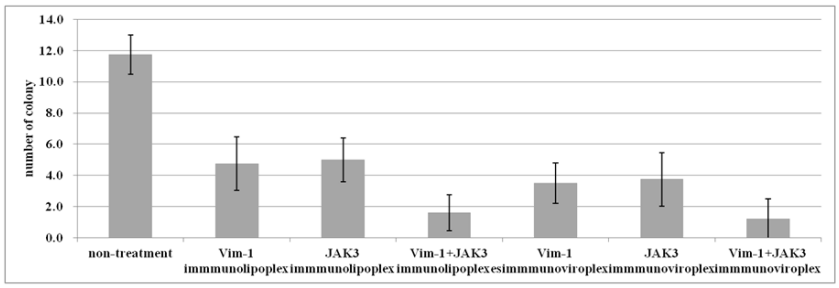

Figure 10. Inhibition of tumor growth and metastasis by intravenous administration of anti-EGFR immunonanoparticles containing vimentin siRNA and/or JAK3 siRNAs.

The anti-EGFR immunonanoparticles containing vementin and/or JAK3 siRNAs were intravenously administered to mice carrying SK-OV-3 tumors. The tumor growth (A) was measured for 37 days and the pulmonary tumor colony (B) was counted on day 46 post tumor innoculation. Solid arrows indicate the administrations of the anti-EGFR immunonanoparticles.

(A) Tumor volume

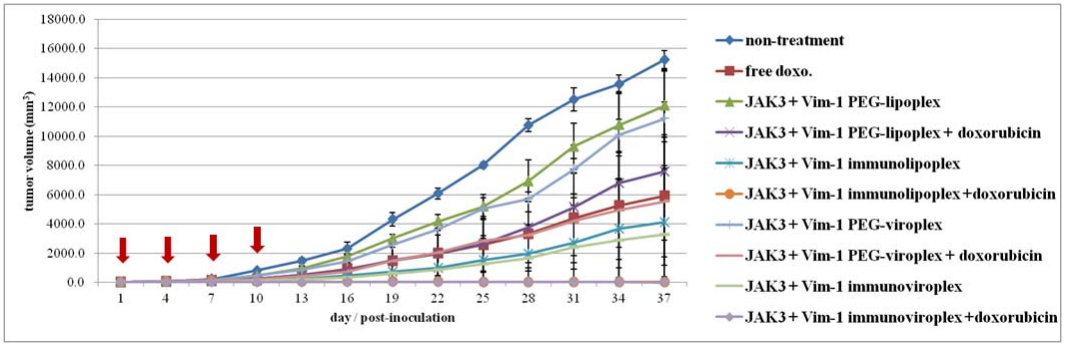

(B) Counting of lung tumor colony

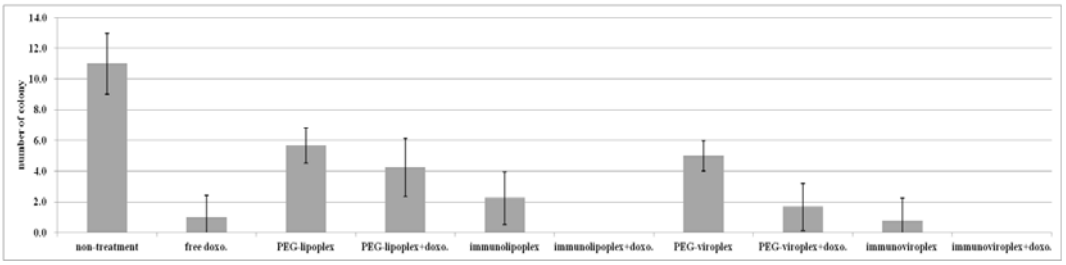

Figure 11. Inhibition of tumor growth and metastasis by intratumoral administration of anti-EGFR immunonano particles containing vimentin and/or JAK3 siRNAs and intravenous adminstration of doxorubicin.

The anti-EGFR immunonanoparticles containing vimentin siRNA and/or JAK3 siRNA were directly administered to SK-OV-3 tumor tissues and doxorubicin was intravenously administer to the same mice. The tumor growth (A) was measured for 37 days and the pulmonary tumor colony (B) was counted on day 46 post tumor innoculation, Solid arrows indicate the administrations of the anti-EGFR immunonanoparticles ad doxorubicin.

Ⅳ. Discussion

Gene therapy with RNA interference (RNAi) technology has been considered to be an innovative procedure to treat numerous cancers (88, 89). Small interfering RNAs (siRNAs) have been known to be a major class of molecules inducing RNAi. Recently, a number of different siRNAs such as VEGF siRNA, survivin siRNA and Bcl2 siRNA have been developed and utilized to treat a variety of cancers (90). However, A major limitation to clinical applications of siRNA is the absence of effective siRNA delivery. To overcome these problems, liposomal gene delivery systems have been improved to provide efficient siRNA delivery to the cytoplasm of intended cells with the least complications (5).

In this study, vimentin and JAK3 siRNAs were loaded in the anti-EGFR immunonanoparticles for anticancer therapy. Vimentin is one of the most widely expressed intermediate filament proteins and essential in maintaining cell adhesion, migration, and survival (91-95). Recently, vimentin degradation has been related to a proapoptotic process that can markedly enhance cell death (96). It is also known that JAK-mediated signaling is important for cell differentiation, proliferation, and survival in mammalian cells (83). The dysregulation of JAK3 induced cancers such as hematological or breast cancers (86). Therefore, inhibition of JAK3 kinase has been reported to be a reasonable strategy for cancer gene therapy (87, 97).

To deliver vimentin and JAK3 siRNA to the cytoplasm of tumor cells, four different types of anti-EGFR immunonanoparticles (immunoliposomes, immunovirosomes, immunolipoplexes, and immunoviroplexes) were prepared. Expectedly all of the anti-EGFR immunonanoparticles exhibited effective cellular binding to EGFR-positive A549 and SK-OV-3 cells. The same systems did not show specific binding to EGFR-negative MCF-7 and B16Bl6 cells, but a certain level of nonspecific binding. In addition, the anti-EGFR immunonanoparticles were able to deliver siRNA specifically to EGFR-positive SK-OV-3 and A549 cells. Meanwhile, the same systems did not show efficient siRNA deliver to the EGFR-negative MCF-7 and B16BL6 cells. Competitive inhibition of their bindings to A549 and SK-OV-3 cells by pretreatment with

free Cetuximab implied EGFR-mediated siRNA delivery of the immunonanoparticles. These results strongly implied that the higher binding and more efficient siRNA delivery to the EGFR-positive cancer cells are due to specific interactions between Cetuximab coupled to nanoparticles and EGFR overexpressed on the cancer cell surface.

The anti-EGFR immunolipoplexes and immunoviroplexes were able to deliver luciferase and vimentin siRNA to the A549 and SK-OV-3 cells, resulting in significant reduction of target gene expression in the cells. However, the same systems showed far less siRNA transfection to MCF-7 and B16BL6 cells, as expected. These results also draw the same conclusion of EGFR-mediated siRNA transfection by the immunonanoparticles.

The anti-EGFR immunolipoplexes and immunoviroplexes were efficiently delivered to SK-OV-3 tumor tissues even though they are positively charged. This implies that PEGylation of the cationic immunolipoplexes and immunoviroplexes (total 4 mol% PEG-PE) may provide adequate steric hindrance to serum proteins, resulting in less taken-up by RES. Presumably, the PEGylated immunolipoplexes and immunoviroplexes were able to circulate long enough to be extravasated to tumor tissues.

Therefore, these two systems containing anticancer vimentin siRNA and/or JAK3 siRNA were carefully prepared and systemically administered to mice carrying tumors. According to the *in vivo* siRNA transfection results, the anti-EGFR immunolipoplexes and immunoviroplexes were able to efficiently deliver the anticancer siRNA molecules to SK-OV-3 tumor tissues, resulting in significant inhibition of tumor progression. Co-transfection of the two anticancer siRNA more effectively inhibited growth and metastasis of the tumors in mice than transfection of either one. The inhibition of tumor progression by the anticancer siRNAs transferred by the anti-EGFR immunonanoparticles was further enhanced by intravenous administration of doxorubicin. Recently, Hu Y. et al also reported enhanced anti-tumoral effect of combinational RNAi gene therapy. They showed that intravenous administration of immunolipoplexes of EGFR siRNA and TERT (telomerase reverse transcriptase) siRNA caused an additive effect on tumor growth inhibition in mice (98).

In this study, some of tumor-carrying mice cotreated with doxorubicin and

the two anticancer siRNAs became cancer-free, complete tumor regression and no pulmonary metastasis. Among the five mice, three mice became cancer-free after cotreatment with doxorubicin and the immunoviroplexes containing vimentin and JAK3 siRNAs. Also, two mice became cancer-free by cotreatment with doxorubidin and the immunolipoplexes containing the two siRNAs. Therefore, at this moment it can be concluded that the anti-EGFR immunoviroplexes are the most efficient EGFR-directed siRNA delivery system among the immunonanoparticles tested. Regarding combination of gene therapy and chemical therapy, an interesting study was reported by Lahat G. et al (99). They showed that cotreatment with anti-angiogenic withaferin-A and liposomes containing vimentin siRNA was able to more effectively inhibit tumor growth than treatment with either one.

This study shows that a rationale of siRNA delivery mediated by specific interactions between EGFR on tumor cell surface and anti-EGFR immunonanoparticles could be realized. Also, this study suggest that these types of anti-EGFR immunonanoparticles could be applicable to EGFR-directed delivery of various functional siRNA molecules for a variety of purposes. In conclusion, the anti-EGFR immunonanoparticles are an improved nonviral siRNA delivery system for transfection to EGFR-expressing cancer cells. Especially, the anti-EGFR immunoviroplexes which are proven to be the most effective transfection system could be widely utilized for clinical applications of RNAi.

Ⅴ. Reference

1. Weir B, Zhao X, Meyerson M. Somatic alterations in the human cancer genome. *Cancer Cell* (2004) 6:433-438.

2. Thomas M, Ge Q, Lu JJ, Chen J, Klibanov AM. Crosslinked small polyethylenimines: While still nontoxic, deliver DNA efficiently to mammalian cells *in vitro* and *in vivo*. *Pharm Res* (2005) 22:373-380.

3. Jang SH, Choi SJ, Oh JH, Chae SW, Nam KH, Park JS, Lee HJ. Nonviral gene delivery to human ovarian cancer cells using arginine-grafted PAMAM dendrimer. *Drug Development and Industrial Pharmacy* (2011) 37:41-46.

4. Ciardiello F, Tortora G. A novel approach in the treatment of cancer: targeting the epidermal growth factor receptor. *Clin Cancer Res* (2001) 7: 2958-2970.

5. Kaneda Y. Update on non-viral delivery methods for cancer therapy: possibilities of a drug delivery system with anticancer activities beyond delivery as a new therapeutic tool, *Expert Opin. Drug Deliv* (2010) 7: 1079-1093.

6. Medina OP, Pillarsetty N, Glekas A, Punzalan B, Longo V, Gönen M, Zanzonico P, Smith-Jones P, Larson SM. Optimizing tumor targeting of the lipophilic EGFR-binding radiotracer SKI 243 using a liposomal nanoparticle delivery system. *Journal of Controlled Release* (2010) 149:292-298.

7. Wan Y, Kim YT, Li N, Cho SK, Bachoo R, Ellington AD, Samir M Iqbal. Surface-Immobilized Aptamers for Cancer Cell Isolation and Microscopic Cytology. *Cancer Res* (2011) 70:9371-9380.

8. Ehrlich P. Collected studies on immunity. John Wiley and Sons, *New York* (1906).

9. Bangham AD. Lipid bilayers and biomembrane. *Annu Rev Biochem* (1972) 41:753-776.

10. Portnoy E, Lecht S, Lazarovici P, Danino D, Magdassi S. Cetuximab-labeled liposomes containing near-infrared probe for *in vivo* imaging. *Nanomedicine* (2011) 7:480-488.

11. Bouche O, Beretta GD, Alfonso PG, Geissler M. The role of antiepidermal growth factor receptor monoclonal antibody monotherapy in the treatment of metastatic colorectal cancer. *Cancer Treat Rev* (2010) 36(Suppl 1):S1-10.

12. Becker JC, Muller-Tidow C, Serve H, Domschke W, Pohle T. Role of receptor tyrosine kinases in gastric cancer: new targets for a selective therapy. *World J Gastroenterol* (2006) 12:3297-3305.

13. Prenzel N, Fischer OM, Streit S, Hart S, Ullrich A. The epidermal growth factor receptor family as a central element for cellular signal transduction and diversification. *Endocr Relat Cancer* (2001) 8:11-31.

14. Mendelsohn J. Targeting the epidermal growth factor receptor for cancer therapy. *J Clin Oncol* (2002) 20:1S-13S.

15. Sato JD, Kawamoto T, Le AD, Mendelsohn J, Polikoff J, Sato GH. Biological effects *in vitro* of monoclonal antibodies to human epidermal growth factor receptors. *Mol Biol Med* (1983) 1:511-529.

16. Goldstein NI, Prewett M, Zuklys K, Rockwell P, Mendelsohn J. Biological efficacy of a chimeric antibody to the epidermal growth factor receptor in a human tumor xenograft model. *Clin Cancer Res* (1995) 1:1311-1318.

17. Baselga J, Pfister D, Cooper MR, Cohen R, Burtness B, Bos M, D''Andrea G, Seidman A, Norton L, Gunnett K, Falcey J, Anderson V, Waksal H, Mendelsohn J. Phase I studies of anti-epidermal growth factor receptor chimeric antibody C225 alone and in combination with cisplatin. *J Clin Oncol*

(2000) 18:904-914.

18. Bonner J A, Raisch K P, Trummell H Q, Robert F, Meredith R F, Spencer S A, Buchsbaum D J, Saleh M N, Stackhouse M A, LoBuglio A F, Peters G E, Carroll W R, Waksal H W. Enhanced apoptosis with combination C225/radiation treatment serves as the impetus for clinical investigation in head and neck cancers. *J Clin Oncol* (2000) 18:47S-53S.

19. Koo OM, Rubinstein I, Onyuksel H. Role of nanotechnology in targeted drug delivery and imaging: a concise review. *Nanomedicine* (2005) 1:193-212.

20. Bohl Kullberg E, Bergstrand N, Carlsson J, Edwards K, Johnsson M, Sjoberg S, Gedda L. Development of EGF-conjugated liposomes for targeted delivery of boronated DNA-binding agents. *Bioconjugate Chem* (2002) 13: 737-743.

21. Li S, Huang L. Nonviral gene therapy: Promises and challenges. *Gene Ther* (2000) 7:31-34.

22. Nicolazzi C, Garinot M, Mignet N, Scherman D, Bessodes M. Cationic lipids for transfection. *Curr Med Chem* (2003) 10:1263-1277.

23. Boussif O, Lezoualc'h F, Zanta MA, Mergny MD, Scherman D, Demeneix B, Behr JP. A versatile vector for gene and oligonucleotide transfer into cells in culture and *in vivo*: Polyethylenimine. *Proc Natl Acad Sci USA,* (1995) 92: 7297-7301.

24. Kichler A. Gene transfer with modified polyethylenimines. *J Gene Med* (2004) 6:S3-10.

25. Sanderson CM, Avalos R, Kundu A, Nayak DP. Interaction of Sendai viral F, HN, and M proteins with Host Cytoskeletal and Lipid Components in Sendai virus-infected BHK cells. *VIROLOGY* (1995) 209:701-707.

26. Wright S, Huang L. *Advanced Drug Deliuery Reviews* (1989) 3:343-3389.

27. Bally MB, Lim H, Cullis PR, Mayer LD. Controlling the drug delivery attributes of lipid-based drug formulations. *J Liposome Res* (1998) 8:299-335.

28. Lundberg B. The solubilization of lipophilic derivatives of podophyllotoxins in submicron sized lipid emulsions and their cytotoxic activity against cancer-cells in culture. *Int. J. Pharmaceut* (1994) 109:73-81.

29. Lundberg BB, Griffiths G, Hansen HJ. Cellular association and cytotoxicity of anti-CD74-targeted lipid drugcarriers in B lymphorna cells. *J Controlled Release* (2004) 94:155-161.

30. Torchilin VP. Liposomes as delivery agents for medical imaging. *Mol Med Today* (1996) 2:242-249.

31. Allen TM. Liposomes-Opportunities in drug delivery. *Drugs* (1997) 54:8-14.

32. Torchilin VP. Polymer-coated long-circulating microparticulate pharmaceuticals. *J Microencapsul* (1998) 15:1-19.

33. Gabizon A, Catane R, Uziely B, Kaufman B, Safra T, Cohen R, Martin F, Huang A, Barenholz Y. Prolonged circulation time and enhanced accumulation in malignant exudates of doxorubicin encapsulated in polyethyleneglycol coated liposomes. *Cancer Res* (1994) 54:987-992.

34. Maruyama K, Yuda T, Okamoto A, Kojima S, Suginaka A, Iwatsuru M. Prolonged circulation time *in vivo* of large unilamellar liposomes composed of distearoyl phosphatidylcholine and cholesterol containing amphipathic poly-(ethylene glycol). *Biochim Biophys Acta* (1992) 1128:44-49

35. Klibanov AL, Maruyama K, Torchilin VP, Huang L. Amphipathic polyethyleneglycols effectively prolong the circulation time of liposomes. *FEBS Lett* (1990) 268:235-237.

36. Maruyama K. PEG-Immunoliposome. *Bioscience Reports* (2002) 22:251-266.

37. Gabizon A, Shmeeda H, Barenholz Y. Pharmacokinetics of pegylated liposomal Doxorubicin: review of animal and human studies. *Clin Pharmacokinet* (2003) 42:419-36.

38. Kang IC, Chung KH, Lee SJ, Yoon YD, Moon HM, Kim DS. Purification and molecular cloning of a platelet aggregation inhibitor from the snake (Agkistrodon halys brevicaudus) venom. *Thromb Res* (1998) 91:65-73.

39. Kim SI, Kim KS, Kim HS, Kim DS, Jang YS, Chung KH, Park YS. Inhibitory Effect of the Salmosin Gene Transferred by Cationic Liposomes on the Progression of B16BL6 Tumors. *CANCER RESEARCH* (2003) 63:6458-6462.

40. Park YS, Kim KS, Lee YK, Kim JS, Baek JY, Huang L. Inhibition of TC-1 Tumor Progression by Cotransfection of Saxitilin an IL-12 Genes Mediated by Lipofection or Electroporation. *Oncology research* (2009) 18:203-212.

41. Nishitani M, Sakai T, Kanayama H, Himeno K, Kagawa S. Cytokine gene therapy for cancer with naked DNA. *Mol Urol* (2000) 4:47-50.

42. Airoldi I, Di Carlo E, Cocco C, Taverniti G, D'Antuono T, Ognio E, Watanabe M, Ribatti D, Pistoia V. Endogenous IL-12 triggers an antiangiogenic program in melanoma cells. *Proc Natl Acad Sci USA* (2007) 104:3996-4001.

43. Sangro B, Mazzolini G, Ruiz J, Herraiz M, Quiroga J, Herrero I, Benito A, Larrache J, Pueyo J, Subtil JC, Olagüe C, Sola J, Sádaba B, Lacasa C, Melero I, Qian C, Prieto J. Phase I trial of intratumoral injection of an adenovirus encoding interleukin-12 for advanced digestive tumors. *J Clin Oncol* (2004) 22:1389-1397.

44. Marshall E. Gene therapy death prompts review of adenovirus vector. *Science (Wash. DC)* (1999) 286:2244-2245.

45. Felgner PL, Tsai YJ, Sukhu L, Wheeler CL, Manthorpe M, Marshall J, Cheng SH. Improved cationic lipid formulations for *in vivo* gene therapy. *Ann NY Acad Sci* (1995) 772:126-139.

46. Liu D, Ren T, Gao X. Cationic transfection lipids. *Curr Med Chem* (2003) 10:1005-1013.

47. Kim HS, Kim JS, Lee YK, Koo KH, Park YS. An efficient liposomal gene delivery vehicle using Sendai F/HN proteins and protamine. *Cancer Gene Therapy* (2008) 15:214-224.

48. Pirollo KF, Xu L, Change EH. Non-viral gene delivery for p53. *Curr Opon Mol Ther* (2000) 2:168-175.

49. Wagner E. Ligand-polycation conjugates for receptor-targeted gene trasfer. IN: Hung, M.C. and Wagner, E. (eds.) Non-viral vector for Gene Therapy. *San Diego: Academic Press* (1999) 208-227.

50. Allen TM, Brandeis E, Hansen CB, Kao GY, Zalipsky S. A new strategy for attachment of antibodies to serically stabilized liposomes resulting in efficient targeting to cancer cells. *Biochim Biophys Acta* (1995) 1237:99-108.

51. Iden DL, Allen TM. *In vitro* and *in vivo* comparision of immunoliposomes made by conventional coupling techniques with those made by a new post-insertion approach. *Biochim Biophys Acta* (2001) 1513:207-216.

52. Lasic DD, Vallner JJ, Working PK. Sterically stabilized liposomes in cancer therapy and gene delivery. *Curr Opin Mol Therpeutic* (1999) 1:177-185.

53. Nam SM, Kim HS, Ahn WS, Park YS. Sterically stabilized anti-G (M3), anti-Le (x) immunoliposomes: targeting to B16BL6, HRT-18 cancer cells. *Oncol Res* (1999) 11:9-16.

54. De Jonge J, Holtrop M, Wilschut J, Huckriede A. Reconstituted influenza

virus envelopes as an efficient carrier system for cellular delivery of small-interfering RNAs. *Gene Therapy* (2006) 13:400-411.

55. Gowhar Shafi, Kaiser Jamil, Atya Kapley, Hemant J Purohit, Mohana Ch Vamsy. RNAi as a novel therapeutic platform technology for oncological solutions. *Biotechnology and Molecular Biology Review* (2008) 4:55-70.

56. de Fougerolles A, Vornlocher HP, Maraganore J, Lieberman J. Interfering with disease: a progress report on siRNA-based therapeutics. *Nat Rev Drug Discov* (2007) 6:443-453.

57. Gao J, Liu W, Xia Y, Li W, Sun J, Chen H, Li B, Zhang D, Qian W, Meng Y, Deng L, Wang H, Chen J, Guo Y. The promotion of siRNA delivery to breast cancer overexpressing epidermal growth factor receptor through anti-EGFR antibody conjugation by immunoliposomes. *Biometerials* (2011) 32: 3459-3470.

58. Baker M. RNA interference: homing in on delivery. *Nature* (2010) 22: 1225-1228.

59. Morille M, Passirani C, Vonarbourg A, Clavreul A, Benoit JP. Progress in developing cationic vectors for non-viral systemic gene therapy against cancer. *Biomaterials* (2008) 29:3477-3496.

60. Oh YK, Park TG. siRNA delivery systems for cancer treatment. *Adv Drug Deliv Rev* (2009) 61:850-862.

61. Tseng YC, Mozumdar S, Huang L. Lipid-based systemic delivery of siRNA. *Adv Drug Deliv Rev* (2009) 61:721-731.

62. Li SD, Chono S, Huang L. Efficient gene silencing in metastatic tumor by siRNA formulated in surface-modified nanoparticles. *J Control Release* (2008) 126:77-84.

63. Li SD, Chen YC. Hackett MJ, Huang L, Tumor-targeted delivery of siRNA by self assembled nanoparticles. *Mol Ther* (2008) 16:163-169.

64. Gao J, Feng SS, Guo Y. Antibody engineering promotes nanomedicine for cancer treatment. *Nanomedicine* (2010) 5:1141-1145.

65. Liu Y, Li K, Liu B, Feng SS. A strategy for precision engineering of nanoparticles of biodegradable copolymers for quantitative control of targeted drug delivery. *Biomaterials* (2010) 31:9145-9155.

66. Mamot C, Drummond DC, Greiser U, Hong K, Kirpotin DB, Marks JD, Park JW. Epidermal growth factor receptor (EGFR)-targeted immunoliposomes mediate specific and efficient drug delivery to EGFR- and EGFRvIII-overexpressing tumor cells. *Cancer Res* (2003) 63:3154-3161.

67. Kim IY, Kang YS, Lee DS, Park HJ, Choi EK, Oh YK, Son HJ, Kim JS. Antitumor activity of EGFR targeted pH-sensitive immunoliposomes encapsulating gemcitabine in A549 xenograft nude mice. *J Control Release* (2009) 140:55-60.

68. Salomon DS, Brandt R, Ciardiello F, Normanno N. Epidermal growth factor-related peptides and their receptors in human malignancies. *Crit Rev Oncol Hematol* (1995) 19:183-232.

69. Bartlett JM, Langdon SP, Simpson BJ. The prognostic value of epidermal growth factor receptor mRNA expression in primary ovarian cancer. *Br J Cancer* (1996) 73:301-306.

70. Nicholson RI, Gee JM, Harper ME. EGFR and cancer prognosis. *Eur J Cancer* (2001) 37:S9-5.

71. Ranson M. For more than just nonsmall cell lung cancer. *Oncologist* (2002) 7:S16-4.

72. Raymond E, Faivre S, Armand JP. Epidermal growth factor receptor tyrosine kinase as a target for anticancer therapy. *Drugs* (2000) 60:S15-3.

73. Mishani E, Hagooly A. Strategies for molecular imaging of epidermal growth factor receptor tyrosine kinase in cancer. *J Nucl Med* (2009) 50:1199-1202.

74. Tolmachev V, Friedman M, Sandström M, Eriksson T, Rosik D, Hodik M, Ståhl S, Frejd F, Orlova A. Affibody molecules for epidermal growth factor receptor targeting *in vivo*: aspects of dimerization and labeling chemistry. *J Nucl Med (*2009) 50:274-283.

75. Gelovani JG. Molecular imaging of epidermal growth factor receptor expressionactivity at the kinase level in tumors with positron emission tomography, *Cancer Metastasis Rev* (2008) 27:645-653.

76. Mishani E, Abourbeh G, Rozen Y, Jacobson O, Laky D, Ben David I, Levitzki A, Shaul M. Novel carbon-11 labeled 4-dimethyl-amino-but-2-enoicacid[4-(phenylamino)-quinazoline-6-yl]-amides: potential PET bioprobes for molecular imaging of EGFR-positive tumors. *Nucl Med Biol* (2004) 31:469-476.

77. Clarke EJ, Allan V. Intermediate filaments: vimentin moves in. *Curr Biol* (2002) 12:R596-598.

78. Evans RM. Vimentin: the conundrum of the intermediate filament gene family. *Bioessays* (1998) 20:79-86.

79. Lahat G, Zhu QS, Huang KL, Wang S, Bolshakov S, Liu J, Torres K, Langley RR, Lazar AJ, Hung MC, Lev D. Vimentin Is a Novel Anti-Cancer Therapeutic Target; Insights from *In Vitro* and *In Vivo* Mice Xenograft Studies. *PLoS ONE* (2010) 5:e10105.

80. Eckes B, Colucci-Guyon E, Smola H, Nodder S, Babinet C, Krieg T, Martin P. Impaired wound healing in embryonic and adult mice lacking

vimentin. *J Cell Sci* (2000) 113:2455-2462.

81. Bargagna-Mohan P, Hamza A, Kim YE, Khuan Abby Ho Y, Mor-Vaknin N, Wendschlag N, Liu J, Evans RM, Markovitz DM, Zhan CG, Kim KB, Mohan R. The tumor inhibitor and antiangiogenic agent withaferin A targets the intermediate filament protein vimentin. *Chem Biol* (2007) 14:623-634.

82. McInroy L, Maatta A. Down-regulation of vimentin expression inhibits carcinoma cell migration and adhesion. *Biochem Biophys Res Commun* (2007) 360:109-114.

83. Wu W, Sun XH. Janus kinase 3: the controller and the controlled. *Acta Biochim Biophys Sin* (2012) 44:187-196.

84. Sun L, Ma K, Wang H, Xiao F, Gao Y, Zhang W, Wang K, Gao X, Ip N, Wu Z. JAK1/STAT1/STAT3, a key pathway promoting proliferation and preventing premature differentiation of myoblasts. *The Journal of Cell Biology* (2007) 179:129-138.

85. Wang K, Wang C, Xiao F, Wang H, Wu Z. JAK2/STAT2/ STAT3 are required for myogenic differentiation. *Journal of Biological Chemistry* (2008) 283:34029-34036.

86. O'Shea JJ, Gadina M, Schreiber RD. Cytokine signaling in 2002: new surprises in the Jak/Stat pathway. *Cell* (2002) 109(Suppl):S121-131.

87. Klink M, Kielbik M, Nowak M, Bednarska K, Sulowska Z. JAK3, STAT3 and CD3-zeta signaling proteins status in regard to the lymphocytes function in patients with ovarian cancer. *Immunol Invest* (2012) 41:382-398.

88. Favaro E, Indraccolo S. Gene therapy of cancer in the clinic: Good news in sight from Asia. *Curr Opin Mol Ther* (2007) 9:477-482.

89. Pirollo KF, Rait A, Zhou Q, Hwang SH, Dagata JA, Zon G, Hogrefe RI,

Palchik G, Chang EH. Materializing the Potential of Small Interfering RNA via a Tumor-Targeting Nanodelivery System. *Cancer Res* (2007) 67:2938-2943.

90. Kim SH, Jeong JH, Lee SH, Kim SW, Park TG. Local and systemic delivery of VEGF siRNA using polyelectrolyte complex micelles for effective treatment of cancer. *Journal of Controlled Release* (2008) 129:107-116.

91. Lane EB, Hogan BL, Kurkinen M, Garrels JI. Co-expression of vimentin and cytokeratins in parietal endoderm cells of early mouse embryo. *Nature* (1983) 303:701-704.

92. Hendrix MJ, Seftor EA, Chu YW, Seftor RE, Nagle RB, McDaniel KM, Leong SP, Yohem KH, Leibovitz AM, Meyskens FL Jr. Coexpression of vimentin and keratins by human melanoma tumor cells: correlation with invasive and metastatic potential. *J Natl Cancer Inst* (1992) 84:165-174.

93. O'ourke NA, Dailey ME, Smith SJ, McConnell SK. Diverse migratory pathways in the developing cerebral cortex. *Science* (1992) 258:299-302.

94. Hendrix MJ, Seftor EA, Chu YW, Trevor KT. Seftor RE, Role of intermediate filaments in migration, invasion and metastasis. *Cancer Metastasis Rev* (1996) 15:507-525.

95. Wang N, Stamenovic D. Mechanics of vimentin intermediate filaments. *J Muscle Res Cell Motil* (2002) 23:535-540.

96. Byun Y, Chen F, Chang R, Trivedi M, Green KJ, Cryns VL. Caspase cleavage of vimentin disrupts intermediate filaments and promotes apoptosis. *Cell Death Differ* (2001) 8:443-450.

97. Kim BH, Min YS, Choi JS, Baeg GH, Kim YS, Shin JW, Kim TY, Ye SK. Benzoxathiol derivative BOT-4-one suppresses L540 lymphoma cell survival and proliferation via inhibition of JAK3/STAT3 signaling. *Exp Mol Med* (2011) 43:313-321

98. Hu Y, Shen Y, Ji B, Wang L, Zhang Z, Zhang Y. Combinational RNAi gene therapy of hepatocellular carcinoma by targeting human EGFR and TERT. *Eur J Pharm Sci.* (2011) 42:387-391

99. Lahat G, Zhu QS, Huang KL, Wang S, Bolshakov S, Liu J, Torres K, Langley RR, Lazar AJ, Hung MC, Lev D. Vimentin is a novel anti-cancer therapeutic target; insights from *in vitro* and *in vivo* mice xenograft studies. *PLoS One* (2010) 5:e10105.

국문 요약

항EGF수용체 면역나노전달체를 이용한 표적 선택적 항암 유전자 전달

연세대학교 대학원
임상병리학과
김 정 석

유전자 치료는 여러 다양한 질환의 치료에 적용이 가능한 효과적인 치료방법이다. 최근 대부분 유전자 치료 연구는 항암치료에 초점이 맞추어져 있으며, 항암 유전자 치료는 항암 유전자(plasmid DNA, micro RNA or small interfering RNA)를 유전자 전달체를 통해 표적 세포로 전달하여 암을 치료하는 것이다. 그러나 이러한 목적으로 사용되는 유전자 전달체는 안전성과 효율성에 개선의 여지가 많다. 비바이러스성 유전자 전달체 중 대표적인 리포솜 유전자 전달체는 다른 유전자 전달체들보다 안정적이고 효율적인 유전자 전달체로 알려져 있다. 또한 바이러스성 전달체에 비해 면역원성이나 감염원성이 낮아 임상적 적용이 용이하다. 리포솜 복합체는 양전하를 띄는 리포솜과 음전하를 띄는 핵산물질(DNA, siRNA 등)이 전기적으로 결합하여 만들어 진다. 그리고 중성이나 음전하를 지니는 리포솜은 체내의 혈청단백들과의 결합 활성이 낮아 체내에서 표적 전달에 장점을 가지고 있다. 여기에 폴리에틸렌글리콜(polyethylene glycol, PEG)을 부착한 리포솜(일명 stealth liposome)은 체내순환을 더 오래 유지할 수 있다. 또한 리포솜의 한 종류인 바이로솜은 다향한 바이러스(influenza, HSV, HIV, Sendai virus 등)의 막단백질을 리포솜에 첨가하여 제조하며, 세포막 부착능이 큰 장점을 가지고 있다. 최근, 이러한 리포솜 유전자 전달체는 세포 및 동물 모델을 이용한 실험에서 과거보다 향상된 표적 특이적 유전자 전달과 생체 내·외의 안정성을 보여주고 있다.

본 연구에서는 다양한 암종에서 과발현을 하여 세포의 성장과 증식 등에 관여하는 상피세포성장인자 수용체 (epithelial growth factor receptor, EGFR)를 표적으로 하는 유전자 전달체를 개발하고자 한다. 우선 EGFR에 특이적인 Cetuximab 항체를 리포솜 표면의 PEG 말단에 부착하여 4 가지 유형의 면역나노입자(항EGFR 면역리포솜, 면역바이로솜, 면역리포솜복합체, 면역바이로솜복합체)를 구성하게 되었다. 세포실험

을 통해 각 면역나노입자들은 EGFR 과발현 암세포(A549, SK-OV-3)에 효율적이고 선택적인 유전자 전달을 보였으나, 대조군 세포(MCF-7, B16BL6)에는 반응하지 않았다. 특히 항EGFR 양이온성 면역바이로솜복합체는 EGFR발현 세포를 대상으로 한 유전자 전달효과가 가장 뛰어났다. 또한 항EGFR 면역나노입자들은 난소암(SK-OV-3) 마우스 모델에서 비표적성인 DMKE/Chol 양이온성 리포솜 복합체보다 종양세포에 선택적이고 효과적인 유전자 전달을 보였다. 따라서 여기에 서로 다른 항암 유전자 IL12와 salmosin 발현용 pDNA를 포획하거나 항암 vimentin siRNA 와 JAK3 siRNA를 포획하였다. 이렇게 항암 유전자가 포획된 항EGFR 면역리포솜 복합체와 항EGFR 면역바이로솜 복합체를 난소암 마우스 모델에 정맥 투여하였다. 또한 별도의 실험에서는 항암제 doxorubicin을 함께 투여하였다. 두 전달체를 통해 마우스에 전달된 IL12와 salmosin 유전자는 효율적으로 발현되어 뚜렷한 항암활성을 보였다. 또한 같은 전달체를 통해 전달된 vimentin siRNA와 JAK3 siRNA도 효율적으로 암의 성장과 전이를 억제하였다. 항암유전자 발현 실험에서나 항암 siRNA 전달실험에서 공통적으로 화학치료 병행이 뚜렷한 치료상승을 나타냈다. 두 유전자 전달체중에 항EGFR 면역바이로솜복합체를 이용한 경우에서 보다 효과적인 유전자 전달과 항암치료활성을 볼 수 있었다. 결론적으로 본 연구를 통하여 개발된 항EGFR 면역유전자 전달체들은 EGFR 선택적인 유전자 전달체로써 사용이 가능하다. 특히 항EGFR 면역바이로솜복합체의 표적세포 선택적 유전자 전달 효과와 항암 치료 효과가 뛰어났다. 또한 유전자 치료와 화학치료가 항암 치료효과를 상승시킬 수 있음을 보여주었다.

Key words : 유전자 치료, 항EGFR 면역유전자 전달체, 면역리포솜, 면역리포솜 복합체, 면역바이로솜, 면역 바이로솜 복합체, 상피세포성장인자 수용체, cetuximab, 센다이 F/HN 단백질, pIL12, pSal, vimentin siRNA, JAK3 siRNA

감사의 글

이 논문이 나오기 전까지 많은 가르침과 조언을 해주신 박용석 교수님께 깊은 감사를 드립니다. 그리고 제가 대학원에 있으면서 많은 가르침을 주신 오옥두 교수님, 김태우 교수님, 김종배 교수님, 이혜영 교수님, 김윤석 교수님, 이기종 교수님께도 진심으로 감사드립니다. 또한 지금은 은퇴하셨지만 양용성 교수님께도 감사의 말씀을 전합니다. 선배이면서 이번 제 논문 때문에 많은 고생을 한 홍성 형님, 학부부터 대학원까지 많은 신경을 써주신 임병혁 선생님께도 감사드립니다. 같은 실험실에서 동고동락하면서 오랫동안 같이 있어준 연경이, 학부시절부터 많은 술을 기울이면서 지낸 화연이, 중간에서 많은 고생을 한 영은이, 이제 갓 들어왔지만 앞으로 고생할 성재와 민우에게도 고맙다는 말을 전하고 싶습니다. 그 외에도 학위 과정동안 많이 힘이 되어준 모든 임상병리학과 및 대학원의 선배님들과 동기들, 후배들에게도 감사의 마음을 전합니다. 이제 졸업을 맞이하면서 그 동안 있었던 즐겁고 행복했던 기억들이 제게 있어 앞으로 사회에서도 좋은 추억으로 남을 것이고, 힘이 될 것 같습니다.

이러한 과정을 마지기까지 가족들이 많은 도움을 주셨다는 생각이 듭니다. 항상 힘들고 어려운 일이 있을 때마다 힘이 되어 준 아버지와 어머니에게 정말 감사드립니다. 그리고 많은 조언을 해준 매형과 누나, 볼 때마다 항상 힘을 준 예쁜 조카들 지원이와 대현이, 그 외에도 제가 이렇게 공부하는데 있어 많은 도움을 주신 친척분들 모두에게 감사를 드리며 작지만 이 논문을 바칩니다.

앞으로 사회에 나가 생활하는데 있어, 이 모든 분들의 도움을 잊지 않고 더욱 정진하기 위해 노력하겠습니다. 학위 과정동안 주신 가르침과 조언들을 잊지 않고 제 마음속에 되새기며 살아갈 수 있도록 하겠습니다. 모든 분들께 감사합니다.

2012년 7월 4일

김정석 드림.